Energy & Buildings 350 (2026) 116550

Contents lists available at ScienceDirect

Energy & Buildings

journal homepage: www.elsevier.com/locate/enb

Invited Review Article

Co-simulation of building energy and geothermal systems: A review

Hamed Yazdani *, Philipp Blum, Kathrin Menberg

Karlsruhe Institute of Technology (KIT), Institute of Applied Geosciences (AGW), Kaiserstraße 12, 76131 Karlsruhe, Germany

ARTICLE INFO

Keywords:
Co-simulation
Model coupling
Building energy
Shallow geothermal systems
Software review

ABSTRACT

Integration of geothermal systems into buildings is imperative for a sustainable energy transition. Coupled simulation of building energy systems and geothermal technologies can support reliable and efficient geothermal-based system design, while ensuring thermal comfort inside the building. While co-simulation has been widely applied, a comprehensive review of existing approaches and applications is still lacking. This study, therefore, reviews co-simulation of building energy and geothermal systems covering modeling techniques, coupling approaches, software options, as well as existing case studies. A total of 141 co-simulation studies were identified, mostly conducted using one single software such as TRNSYS (58 %), EnergyPlus (9 %), IDA ICE (8 %) and Modelica (5 %) by incorporating simplified semi-analytical geothermal models. Only few studies coupled a building energy tool with a high-fidelity physical model of the subsurface for co-simulation (< 10 %). Studies mainly focused on borehole heat exchangers (BHE) (65 %), followed by borehole thermal energy storage (BTES) (19 %), ground heat exchangers (GHE) (8 %), aquifer thermal energy storage (ATES) (3 %) and energy piles (EP) (2 %). Over 80 % of research investigated residential, commercial and institutional buildings, largely for heating applications. Co-simulation revealed high potential of geothermal systems in buildings, with COP of 4 ± 1, discomfort times of 6 % ± 4 %, payback period of 14 ± 9 years, and CO_2 savings of 40 % ± 27 %. The literature review showed an evolution from early feasibility analyses to detailed physics co-simulation and hybrid geothermal energy systems. Several opportunities are highlighted for future research in the field regarding software coupling, geothermal model validation and system design. Specifically, creating a co-simulation framework for optimal design of building integrated geothermal systems is the key opportunity for advancing geothermal technology application.

1. Introduction

Clean energy investments have been effective in damping increase of CO_2 levels. However, emissions continue to rise on a global scale, mainly due to growing energy consumption. Currently, the building sector is responsible for over one-third of global final energy consumption, accounting for 26 % of energy-related emissions [1]. Implementing passive strategies to reduce building energy demands, along with replacing conventional supply systems with clean and energy-efficient technologies, is essential for decarbonizing the building sector.

Heat pumps (HP) offer a large potential for energy transition in the building sector by supplying low-emission heating and cooling. HPs currently provide around 10 % of energy demand [1]. Yet installations would have to triple over the next five years in order to meet the Net Zero Emissions (NZE) goal by 2050 [1].

Geothermal heat pumps (GHP) and air-source heat pumps (ASHP), which exploit underground energy and ambient air, respectively, are common types of HPs. GHPs were shown to be superior to ASHPs in terms of long-term economic benefits [2], superior life cycle performance [3], alleviating subsurface urban heat island [4], and reducing peak electricity grid loads [5,6]. Shallow geothermal energy is also considered a key component in 5th-generation district heating and cooling networks, operating close to or lower than ambient temperature [7,8]. Although high installation costs remain a challenge for widespread application of geothermal-based systems [9]; integrating them with other energy systems can improve their profitability [10].

Shallow geothermal systems can be classified into closed and open systems. In closed systems, heat transfer occurs through the circulation of a working fluid within buried pipes, while open systems use groundwater directly as the heat transfer medium. Horizontal ground heat exchangers (GHE) and vertical borehole heat exchangers (BHE), both also called ground-source heat pumps (GSHP), as well as energy piles (EP) are common closed systems, while groundwater heat pumps (GWHP) are common open system geothermal technology. All geothermal systems can be intentionally charged for seasonal energy

* Corresponding author.
E-mail address: hamed.yazdani@kit.edu (H. Yazdani).

https://doi.org/10.1016/j.enbuild.2025.116550
Received 16 July 2025; Received in revised form 12 September 2025; Accepted 4 October 2025
Available online 10 October 2025

Nomenclature

Abbreviations

AHU	Air handling unit
API	Application programming interface
ASHRAE	American Society of Heating, Refrigerating and Air-Conditioning Engineers
ATES	Aquifer thermal energy storage
BBD	Box–Behnken design
BHE	Borehole heat exchanger
BPNN	Back-propagation neural network
BTES	Borehole thermal energy storage
CHP	Combined heat and power
CLI	Command-line interface
COMFIE	Calcul d'Ouvrages Multizones Fixé à une Interface Experte
COP	Coefficient of performance
CTF	Conduction transfer function
DH	District heating
DGC	Direct ground cooling
DHW	Domestic hot water
DSHP	Dual source heat pump
DST	Duct ground heat storage
DVGW	Deutscher Verein des Gas- und Wasserfaches
EED	Earth Energy Designer
EHP	Electric heat pump
EP	Energy pile
FC	Fuel cell
FCS	Finite cylindrical source
FDM	Finite difference method
FEM	Finite element method
FVM	Finite volume method
GA	Genetic algorithm
GHE	Ground heat exchanger
GHP	Geothermal heat pump
GSHP	Ground source heat pump
GUI	Graphical user interface
HSRM	Hybrid step response model
HVAC	Heating, ventilating and air-conditioning
ICE	Internal combustion engine
ILS	Infinite line source
LCC	Life cycle cost
LTG	Long-term *g*-function
MFLS	Moving finite line source
MPC	Model predictive control
MRST	MATLAB Reservoir Simulation Toolbox
N/A	Not known
NC	Not considered
NGB	Natural gas-fired boiler
NPV	Net present value
ORC	Organic Rankine cycle
PBD	Platform-based design
PCM	Phase change material
PVT	Photovoltaic thermal
RBC	Rule-based control
RPC	Remote procedure call
RSM	Response surface methodology
SE	Stirling engine
SPF	Seasonal performance factor
STC	Solar thermal collector
STG	Short-term *g*-function
TAB	Thermally activated building
TCP/IP	Transmission control protocol/internet protocol
TESPy	Thermal engineering systems in Python
TRM	Thermal resistance model
TRCM	Thermal resistance capacitance model
WPB	Wood pellet boiler
WT	Wind turbine
1D	One-dimensional
2D	Two-dimensional
3D	Three-dimensional

Variables

C	Volumetric heat capacity
h	Hydraulic head
k	Thermal conductivity
$\boldsymbol{K}$	Hydraulic conductivity tensor
P	Sink/source power
q	Heat flux
$\boldsymbol{q}$	Flow flux vector
Q	Thermal load
S	Specific storage
t	Time
T	Temperature
$\dot{V}$	Volumetric flow rate
W	Work power
y	Simulation output

Subscripts

b	Building
$disp$	Dispersion
ext	External
f	Fluid
g	Ground
GWF	Groundwater flow
i	Inlet
int	Internal
o	Outlet
m	Porous medium
N	Time step
s	Subsurface
t	Thermal
w	Groundwater

Superscripts

k	Iteration number

storage or for replenishing the ground temperature. The most common closed and open underground thermal energy systems (UTES) are borehole thermal energy storage (BTES) and aquifer thermal energy storage (ATES) [11,12].

There is ample literature on the fundamentals of geothermal energy systems [13–15], testing and performance analysis [9,16–18], technological advances [19–23], policy aspects [24–26], modeling approaches [27–29], geothermal potential [11,30] and applications for heating and cooling in the building sector [31–34]. However, there are few studies that review co-simulation of building energy and geothermal technologies. Do & Haberl [35] presented multiple GSHP models along with software for whole-building energy simulation including TRNSYS, EnergyPlus, DOE-2, eQUEST and EnergyGauge USA. More recently, Lyden et al. [36] reviewed modeling tools for co-simulation of BTES and ATES with a focus on integrating seasonal thermal energy storage into district-scale smart energy systems. A structured review on co-simulating building energy and various geothermal systems is still lacking. Such a review study is essential as modeling and simulation play a significant role in the integration of GHPs into buildings by improving system performance and efficiency, as well as reducing installation and operational costs [37,38].

The objective of this study is therefore to review co-simulation of building energy and geothermal systems, focusing on modeling techniques, coupling approaches, software options and applications, along with highlighting challenges and providing an outlook to promote future research in the field. The rest of this study is structured as follows: Section 2 describes governing equations for building energy and geothermal systems modeling. Section 3 introduces co-simulation concepts and commonly used software tools. Section 4 reviews co-simulation case studies and identifies research trends. Section 5 discusses software and models used for co-simulation in the literature. Section 6 presents current challenges. Finally, section 7 concludes with the study findings, knowledge gaps, as well as recommendations.

2. Physics for modeling building energy and shallow geothermal systems

Fig. 1 summarizes the physics involved in modeling building energy and common shallow geothermal systems. Conduction, convection and radiation from different building components determine thermal loads required to maintain comfortable conditions inside the building. Heating, ventilation, and air conditioning (HVAC) systems, which are used to supply those thermal loads, are typically connected to a GHP operating based on the refrigeration cycle. This cycle consists of four basic thermodynamic processes: compression, condensation, expansion and evaporation. On the source (external) side, the GHP is connected to a closed or open geothermal system, which is modeled by accounting for different heat transfer mechanisms in the subsurface such as axial, lateral and land surface heat fluxes, as well as advection by groundwater flow (Fig. 1). The following subsections describe above-ground and subsurface models in more detail.

2.1. *Building energy modeling*

This section discusses energy modeling techniques for the building envelope, GHP, integrated energy systems and control strategies.

2.1.1. *Building envelope*

There are several standards for calculating building thermal loads such as the international ISO 13790 [39], the American ANSI/ASHRAE Standard 140–2023 [40] and the European EN 15265 [41], which adopt various formulations and techniques.

According to the energy balance, total building thermal load (Q_b) can be evaluated as the sum of internal ($Q_{b,int}$) and external ($Q_{b,ext}$) loads [42,43]:

$$Q_b = Q_{b,int} + Q_{b,ext}. \quad (1)$$

The internal loads can be obtained from different heat transfer processes inside the building thermal zones:

$$Q_{b,int} = q_{ceiling} + q_{floor} + q_{partition} + q_{zones} + q_{surf} + q_{light} + q_{equipment} + q_{occupants}, \quad (2)$$

where $q_{ceiling}$, q_{floor} and $q_{partition}$ are the conductive heat fluxes through the

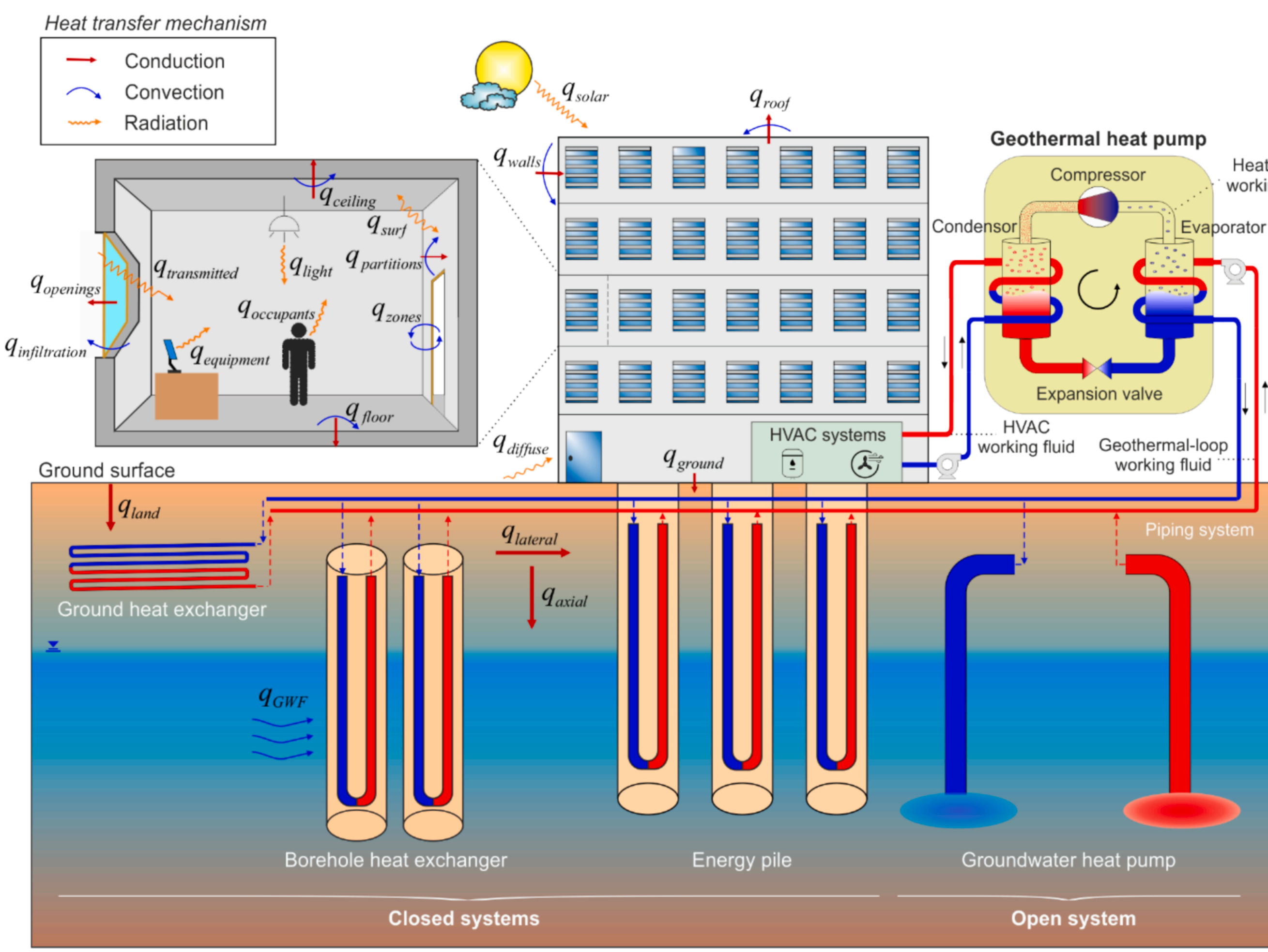

Fig. 1. Fundamental physics of the building energy and subsurface including basic closed and open shallow geothermal systems.

ceiling, floor and interior partitions, respectively. q_{zones} represents the convective heat flux from air exchange between zones. q_{surf} is the radiative heat exchange between zone surfaces, while q_{light}, $q_{equipment}$ and $q_{occupants}$ are the internal gains from lighting, equipment and occupants, respectively.

Similarly, external loads can be calculated using Eq. (3):

$$Q_{b,ext} = q_{roof} + q_{ground} + q_{walls} + q_{openings} + q_{infiltration} + q_{solar} + q_{diffuse} + q_{transmitted}, \quad (3)$$

where q_{roof}, q_{ground}, q_{walls} and $q_{openings}$ are conductive heat fluxes through the roof, ground floor, external walls and openings, respectively. $q_{infiltration}$ refers to the convective heat flux from air exchange between building zones and the ambient environment. q_{solar} is solar radiation, $q_{diffuse}$ includes reflected solar irradiance, as well as radiation from the surroundings (e.g., ground and adjacent buildings), and $q_{transmitted}$ is radiative heat flux passed through openings.

Various models exist for calculation of the above-mentioned heat fluxes [44]. Along with the detailed physics-based heat balance approach (white-box), reduced order models (gray-box) [45] and machine learning techniques (black-box) [46] are available for fast thermal load estimation.

2.1.2. Geothermal heat pump

The performance of GHPs is typically measured by the coefficient of performance (COP) [47]:

$$COP = \frac{Q_b}{W}, \quad (4)$$

where W is electric power consumption. According to the energy balance of GHP, ground thermal load (Q_g) is expressed in Eq. (5) [47]:

$$Q_g = \begin{cases} Q_b - W & \text{heating}, \\ Q_b + W & \text{cooling}. \end{cases} \quad (5)$$

By combining Eqs. (4) and (5), ground load can be derived as a function of building energy demand and COP:

$$Q_g = \begin{cases} Q_b\left(1 - \dfrac{1}{COP}\right) & \text{heating}, \\ Q_b\left(1 + \dfrac{1}{COP}\right) & \text{cooling}. \end{cases} \quad (6)$$

Also, based on energy conservation for the subsurface system, inlet ($T_{f,i}$) and outlet ($T_{f,o}$) temperatures of working fluid in the ground-loop are related according to Eq. (7) [48]:

$$T_{f,o} = \begin{cases} T_{f,i} + \dfrac{Q_g}{C_f \dot{V}} & \text{heating}, \\ T_{f,i} - \dfrac{Q_g}{C_f \dot{V}} & \text{cooling}, \end{cases} \quad (7)$$

where C_f and $\dot{V}$ are the volumetric heat capacity and flow rate of heat carrier fluid, respectively.

There are different mathematical models for COP estimation:

Constant

This is the simplest model, where the COP is assumed to remain constant during operation, based on the assumption of an unlimited source capacity. While this model requires minimal computational effort, it neglects the effects of transient building loads, limiting its applicability for detailed performance analysis. Therefore, it should be used cautiously and only in cases where short-term dynamic effects can be ignored (e.g., in the preliminary design of seasonal energy storage applications) [49].

Regression

Regression (equation-fit) models predict COP as a function of load- and source-side conditions (temperature, part load ratio, etc.) by curve fitting to experimental or manufacturer's performance data. They are widely used in building energy modeling tools due to high accuracy and low complexity. Several mathematical models with linear and nonlinear regression are available for predicting COP [50,51]. However, regression models are often limited to a specific HP model, require extrapolation outside reported operating ranges (off-design conditions), can be unreliable with small catalogue datasets, and are highly dependent on manufacturer data of uncertain origin [50].

Thermodynamic

Thermodynamic models employ mathematical representations of each component (compressor, condenser, expansion valve and evaporator) in the HP cycle to determine the COP. They can be divided into steady-state and transient models. The former use simplified equations to model the refrigerant cycle based on several assumptions (e.g., fully saturated phases and negligible pressure losses), while the latter employ detailed dynamic models that can capture transient effects, making them suitable for system control design and fault diagnosis [52]. Despite high potential, widespread application of thermodynamic models is limited because of high complexity, detailed operational input data requirements and computational cost [53].

Machine learning

Machine learning (ML) methods can predict COP by training on a dataset without requiring any physical information about the HP. Recently, various ML techniques have been used to predict the COP of GHP, more commonly artificial neural networks [54], random forest [55], support vector machine [56] and decision tree ensemble [57]. While they offer great potential for performance prediction of complex physical systems, they have lower explainability and may produce spurious or accidental results [58]. Also, their prediction accuracy and computational cost are highly dependent on the training model employed [57,59].

2.1.3. System components and control

Energy simulation facilitates analyzing the application of various components in buildings [60]:

- *Thermal* (solar thermal collectors (STC), phase change materials (PCM), district heating, chillers, dry coolers, etc.)
- *Electrical* (photovoltaic (PV), wind turbines (WT), fuel cells (FC), batteries, etc.)
- *Thermo-electrical* (photovoltaic thermal (PVT), combined heat and power (CHP) technologies like internal combustion engines (ICE) and organic Rankine cycles (ORC), etc.)

The energy flow management for these components is typically conducted using rule-based controllers (RBC) or model predictive controllers (MPC). RBC employs fixed, pre-set rules for managing energy flow between components, offering simple implementation and fast solutions. MPC, on the other hand, generates control commands by applying a predictive model over a finite time horizon to optimize the current and future behaviors of the system. Recently, MPC has become popular for designing control strategies in various building applications due to its significant potential for energy cost savings [61,62].

2.2. Subsurface modeling

Thermo-hydraulic modeling of the subsurface for geothermal systems is mostly performed based on the governing equations of porous media [63,64]. Heat transport considering conduction, groundwater advection and mechanical dispersion can be expressed as follows:

$$\frac{\partial(C_m T)}{\partial t} = \nabla \bullet \left[k_m + k_{disp} \nabla T\right] - \nabla \bullet (C_w \boldsymbol{q} T) + P_t, \tag{8}$$

where T is temperature, C_m and k_m are the volumetric heat capacity and thermal conductivity of porous medium, respectively, k_{disp} is the dispersion thermal conductivity, C_w is the volumetric heat capacity of groundwater, $\boldsymbol{q}$ is flow flux vector and P_t is the thermal production/sink term.

Also, fluid (groundwater) flow equation based on Darcy's law is formulated in Eq. (9):

$$S\frac{\partial h}{\partial t} = \nabla \bullet [\boldsymbol{K} \nabla h] + P_f, \tag{9}$$

where h is hydraulic head, S is specific storage coefficient, $\boldsymbol{K}$ is hydraulic conductivity tensor and P_f is fluid production/sink term.

While this is the most common approach for representing the subsurface in applications of shallow geothermal energy systems for buildings, there are also models for incorporating solid mechanics and chemical reactions, as well as fractured network in subsurface using the cubic law [65].

3. Co-simulation approaches and software

This section introduces a concept for categorizing co-simulation approaches by model coupling, followed by an analysis of corresponding building and subsurface software packages along with presenting available coupling options.

Existing simulation approaches specifically for building energy and geothermal systems can be grouped into following categories (Fig. 2):

- *Separate simulation*
- *Co-simulation using single software*
- *Co-simulation using multiple software (software coupling)*

In the separate simulation case, building energy and geothermal systems are simulated independently, with the building thermal loads serving as boundary conditions for the subsurface simulation (Fig. 2a). Real-time analysis of the whole building–geothermal system is not feasible, as the building energy and subsurface models are not simulated concurrently. In spite of limitations due to the static nature of this coupling approach, many studies adopt separate simulation to estimate energy performance of geothermal systems and to analyze subsurface temperature changes [66–71].

Co-simulation involves dynamic coupling of both building and geothermal models throughout whole simulation time. Energy, economic, environmental, and exergy (4E) analyses, as well as thermal comfort assessments, are possible because of a holistic modeling approach. Co-simulation also facilitates analyzing geothermal-based hybrid energy systems and real-time analysis for designing physics-based controllers [72–74]. Given its significant potential, co-simulation is increasingly adopted in multi-physics fields for a wide range of building energy and geothermal applications [75,76].

Several energy simulation tools include both building and geothermal models for co-simulation (e.g., TRNSYS, EnergyPlus and Modelica) (Fig. 2b). However, these software, also known as whole-building tools, typically adopt a simplified model for the subsurface

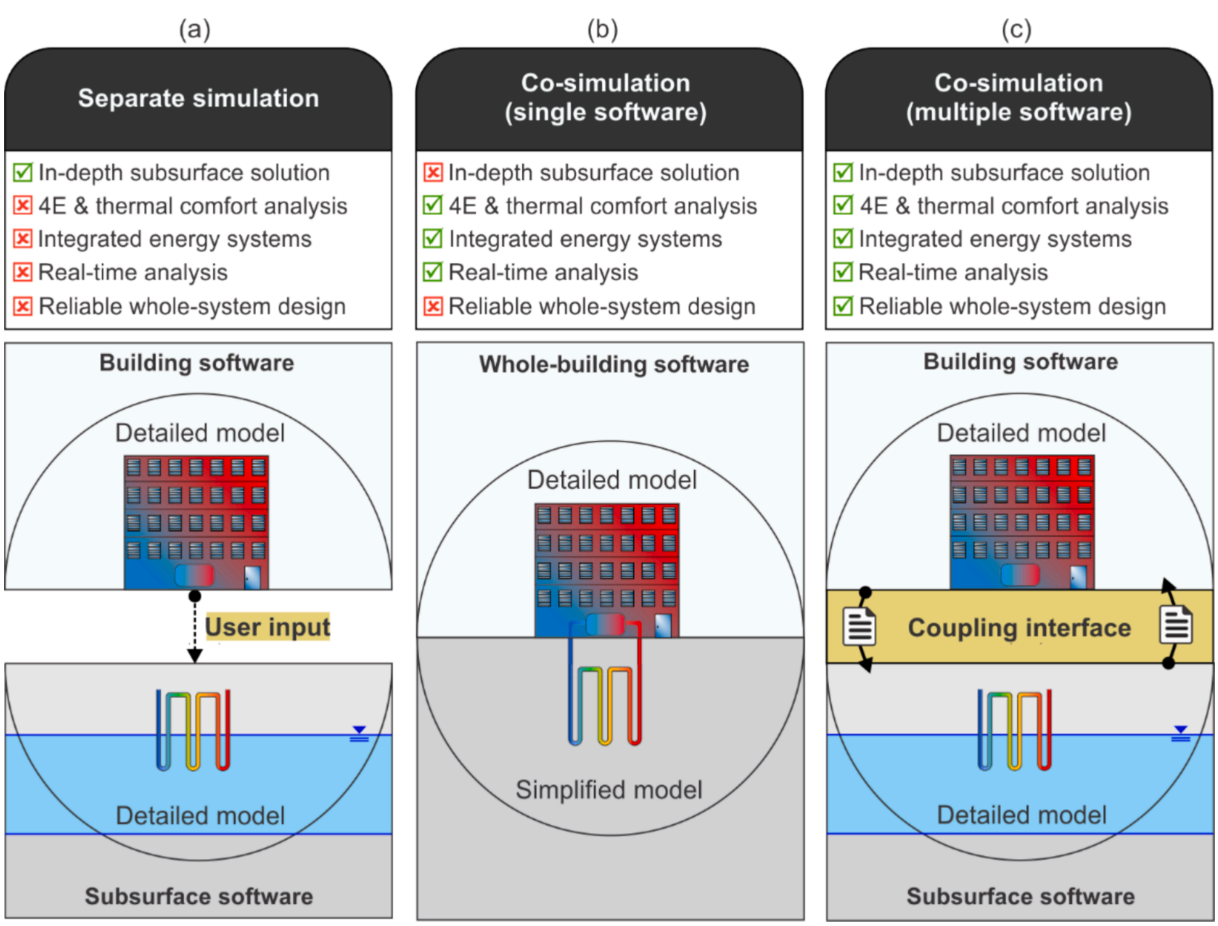

Fig. 2. Simulation of building energy and geothermal systems: (a) separate simulation, (b) co-simulation using a single software and (c) co-simulation using two or more specialized software.

and are limited to specific geothermal systems, mostly BHE (see Appendix A).

Co-simulation can also be performed using multiple software by coupling specialized building energy and subsurface tools (Fig. 2c). This approach not only maintains all the benefits of whole-building energy tools, but also enables detailed subsurface modeling for various geothermal systems and therefore facilitates reliable design of the overall system based on a high-fidelity model. However, it often comes with an increased computational cost and potential errors [77].

3.1. Co-simulation techniques

Fig. 3 illustrates general techniques for co-simulation in a multi-physics system (Figs. 2b and c). Models can be coupled using strong (governing equations) [78] and weak (discrete variables) interfaces [79] (Fig. 3a). In the strong coupling approach, a single solver can be used to perform co-simulation. The discrete variable approach, on the other hand, requires at least two solvers, which increases computational time and numerical errors. Nevertheless, it is the most common approach for

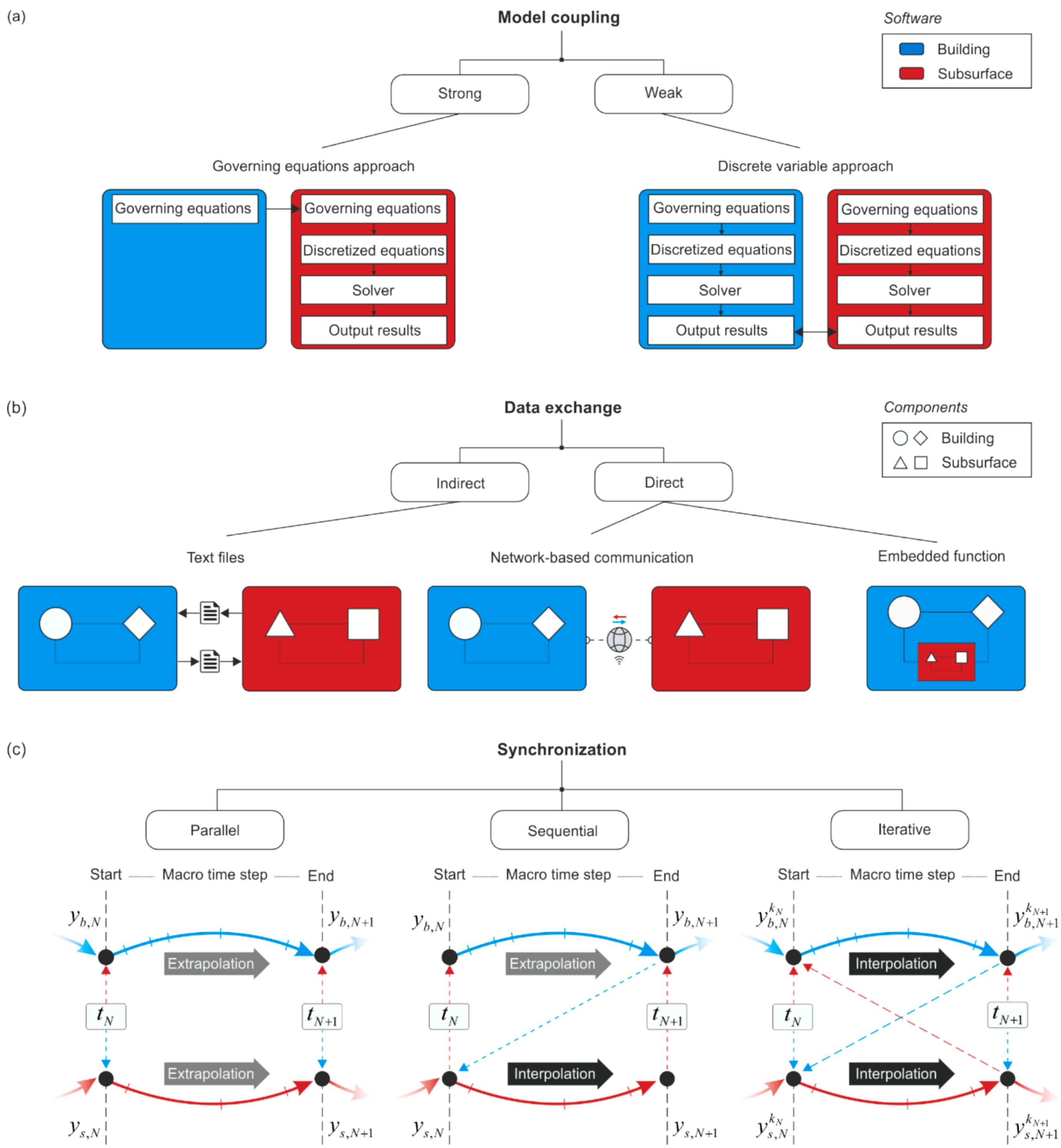

Fig. 3. Concepts of multi-physics co-simulation: (a) general coupling methods, (b) data exchange techniques and (c) synchronization schemes. Data exchange and synchronization apply only to weak coupling.

co-simulation of building energy with geothermal systems.

Weak coupling requires data exchange between software for co-simulation (Fig. 3b). The simplest data exchange approach is to read and write text files in the workspace without any direct interaction between software. This method involves creating additional files and format change during co-simulation, which increases the overall simulation time. Alternatively, data can be exchanged directly between software tools using network communication or calling an embedded function. Network communication involves establishing a client–server architecture in which coupled software exchange information by sending and processing requests remotely based on internet protocols. Remote procedure call (RPC) and transmission control protocol/internet protocol (TCP/IP) are commonly adopted frameworks for enabling data exchange in co-simulation [80–82]. In the embedded function approach, one software is encapsulated in a master software like a dynamic linked component, and data is exchanged by calling a local function. Functional mock-up interface (FMI) standard, for instance, can facilitate dynamic model exchange between software tools [83]. Application programming interface (API) can be used for creating and adapting these linked blocks [84]. Although direct data exchange is more advanced than the indirect method, it requires complex programming and depends on the extensibility potential of the corresponding software. For instance, FMI exists for only a few programming languages, may require specific licenses, and could contain malicious code, which hinders sharing of simulation models across tools. On the other hand, network-based communication tools (i.e., RPC and TCP/IP) provide greater flexibility for data exchange between various simulators, but they require manual synchronization planning, error handling and interface consistency, which can be error-prone and time-consuming [85].

A synchronization scheme is also necessary in the case of weak coupling (Fig. 3c). Various techniques are available with different run-time and accuracies including parallel, sequential and iterative synchronization. The parallel scheme reduces co-simulation time by enabling simultaneous simulation of the building and subsurface software, but it increases transmission error per communication (macro) time steps due to data extrapolation. Sequential synchronization lowers error by interpolating building data for subsurface simulation, but inaccuracies remain as building simulation outputs (e.g., injection temperature and mass flux) are considered constant during subsurface simulation (quasi-dynamic coupling). Iterative synchronization offers the least error, comparable to fully-dynamic (strong) coupling, for an equal communication time step, with the highest computational cost. However, it is possible to achieve more accurate co-simulation results through parallel synchronization with small communication time steps, under a fixed total simulation time constraint. Therefore, devising an optimal coupling approach is essential to balance computational cost and accuracy in a co-simulation.

3.2. Software for building energy modeling

Table 1 compares the features of building energy software that are common for co-simulation. In the following, the capabilities of each software are summarized. Also, a comprehensive list of available geothermal models with solution techniques in these tools is provided in Appendix A.

TRNSYS

TRNSYS is a modular simulation environment widely used for hybrid energy systems modeling due to an abundant number of built-in components (so-called Types) [86]. TRNSYS also allows developing new modules with special functionality using FORTRAN and C codes, based on its suite of tools like TypeStudio. It has advanced and simplified options for thermal load calculation along with detailed building envelope model and daylight illuminance library. It includes several models for GHE, BHE, EP and ATES (Appendix A). The main merits of TRNSYS are its flexibility, extensibility, and suitability for system-level integration studies involving multiple energy technologies [87]. However, traditional load-based controllers and simple regression GHP models are limitations of TRNSYS, making it less suited for studies requiring advanced control strategies.

EnergyPlus

EnergyPlus is an open-source, comprehensive software package for building envelope modeling, thermal load and daylight illuminance calculations [88]. It also provides several advanced semi-analytical models for GHE and BHE simulations. EnergyPlus is particularly well adapted for detailed building-scale studies where the focus is on envelope performance, HVAC operation and energy efficiency analysis [89,90]. However, it has constraints in terms of district-scale analysis, application of real-world controllers and innovative piping systems for simultaneous heating and cooling [91]. Furthermore, it lacks any available models for EP and ATES simulations.

IDA ICE

IDA Indoor Climate and Energy (IDA ICE) is a commercial software based on the neutral model format (NMF) language [92]. It adopts advanced models for thermal load calculation with daylight extension integrated into a comprehensive library of energy systems and plants. IDA ICE has shown strong applicability in building–geothermal design studies and indoor thermal comfort assessments [93,94]. It can only model closed systems GHPs using a regression-based approach, control systems focus on building components (e.g., terminal units, windows and lights), and is rarely coupled with tools like GenOpt for system optimization [95].

Modelica

Modelica is an object-oriented, equation-based, modeling language with Dymola and OpenModelica serving as commercial and free front-ends, respectively [96]. Modelica is widely used for multi-domain modeling in various engineering fields [97]. It allows development of physics-based control strategies to advance building digitalization by simulating real-world controllers based on temperature measurements. Numerous coupling and solver options are further notable strengths. Limited and inefficient building envelope models and HVAC components, as well as lack of daylight calculation tools are the main drawbacks for building energy modeling using Modelica, although they are some recent efforts for improvements [91].

Table 1
Comparison of building energy modeling software regarding different aspects. Level of capability is indicated by the number of ● symbols: basic (●), moderate (●●) and advanced (●●●).

	TRNSYS	EnergyPlus	IDA ICE	Modelica	Simulink	DOE-2	ESP-r	COMFIE	TESPy
Building	●●●	●●●	●●●	●●○	●●○	●●○	●●○	●○○	○○○
Geothermal heat pump	●●○	●●○	●○○	●○○	●○○	●○○	●○○	○○○	●●○
System components and control	●●○	●●○	●●○	●●●	●●○	●○○	●○○	●○○	●●○
Coupling	●●●	●●●	●○○	●●●	●●●	●○○	●●○	●○○	●●●

Simulink

There are four well-known toolboxes developed in MATLAB/Simulink for building performance simulation: CARNOT [98], carnotUIBK [99], HAMBASE [100], and ALMABuild [101]. These tools have limited functionality in thermal load calculation [44], as well as GHP and energy system modeling. However, discrete and continuous solvers, extendibility and abundant coupling options are main advantages of these tools linked to the Simulink object-oriented language. Therefore, they are well-suited for performing co-simulation and control studies [102,103].

DOE-2

DOE-2 is a building energy and cost analysis tool [104]. It uses surface heat transfer and conduction transfer function for thermal load calculation, however it cannot model air heat balance within thermal zones [105]. GHPs are modeled using a regression-based approach as function of part load ratio, and only few HVAC components (e.g., cooling tower, chiller and boiler) can be integrated in building using empirical formulae. Also, its solver cannot couple equations; loads, systems and plants modules can only be simulated sequentially [106]. While it allows customization by user functions, no co-simulation with software coupling has been reported [105]. DOE-2 engine is incorporated into several building energy analysis programs due to its compatibility with building information modeling (BIM) tools [107,108].

ESP-r

ESP-r is an open-source package for energy and acoustic performance simulation of buildings with basic HVAC and electrical components [109]. Although it facilitates modeling of multi-zone buildings with inter- and intra-zone airflow, its energy simulation engine is less advanced compared to TRNSYS and EnergyPlus [110]. Specifically, ESP-r/HOT3000 module can model GHP [111] and STC [112] in buildings. Recently, the integration of ESP-r with digital twins and building decision-making tools has gained attention [113].

COMFIE

COMFIE is primarily designed for fast calculation of thermal loads and comfort assessments in multi-zone buildings based on a simplified reduced order model (modal analysis), which is widely used in France [114]. It has a modular design created with the Delphi object-oriented language, which allows implementing new components and coupling with specific software that supports the Delphi interface. For instance, building energy models in COMFIE are coupled with microclimate and optimization tools [115,116]. Nevertheless, it has insufficient capabilities for system-level simulation.

TESPy

TESPy is a Python toolkit designed for performance simulation of thermal energy plants [117]. It enables simulating HPs, district heating and CHP technologies, yet lacks the capability to model building thermal loads or geothermal systems. TESPy can perform thermodynamic analysis of HPs and thermo-hydraulic simulation of fluid networks, making it ideal for modeling large GHPs with complex piping systems. Although it is primarily based on steady-state analysis and single-phase behavior, its open-source object-oriented structure allows system extensions and advanced control implementation. However, TESPy is prone to convergence challenges, especially at extreme or rapidly changing operating conditions [118,119].

3.3. Software for subsurface physical processes

A variety of numerical tools is available for detailed analysis of the subsurface. Table 2 lists numerical software commonly applied to geothermal systems. Most packages employ finite volume method (FVM) or finite element method (FEM) with a graphical user interface (GUI) to facilitate simulation, except for MODFLOW and TOUGH that adopt finite difference method (FDM) and command-line interface (CLI), respectively.

ANSYS Fluent, COMSOL, FEFLOW and TOUGH are the pioneering tools for geothermal numerical modeling; however, they are commercial products, which makes their codes less transferable for widespread use. More recent programs like MATLAB Reservoir Simulation Toolbox (MRST), OpenGeoSys (OGS), as well as MODFLOW are free and open-source tools, which also possess great potential for subsurface simulation. Specifically, MSRT is a research package offering extensive computational techniques and physical models with data sets for reservoir simulation. OGS is an open-source project written in C++ for simulating thermal, hydrological, mechanical, and chemical processes which can be solved in a fully coupled manner or in a sequential way. Additionally, MODFLOW includes Fortran-based, object-oriented models for groundwater flow, as well as multi-species solute transport (MT3DMS) [120] and heat flow (SEAWAT) [121].

3.4. Coupling interfaces for different software packages

In general, software can be coupled using built-in or user-developed tools. For instance, software tools supporting FMI standard are capable of exporting models for use in a corresponding program as embedded functions, commonly known as functional mock-up units (FMU), which are reported to exist for over 200 tools. Furthermore, Building Controls Virtual Test Bed (BCVTB) program allows coupling various software including EnergyPlus, Matlab/Simulink, Modelica, ESP-r, TRNSYS, as well as FMUs [129]. Similarly, Spawn engine facilitates co-simulation of building energy model in EnergyPlus (OpenStudio) with HVAC and control libraries in Modelica [91].

In addition to built-in tools, users can couple software through their programming interfaces. TRNSYS–FEFLOW [130], Modelica–OGS [131], Modelica–TOUGH [132], TESPy–OGS [133], Python–MODFLOW [134] and COMFIE–MATLAB [135] were successfully coupled in such way. Furthermore, some software tools can be coupled through a third-party program. For instance, Dahash et al. [136] coupled COMSOL–Dymola (Modelica) using both MATLAB and TSIC Suite, while Ferroukhi et al. [137] linked TRNSYS and COMSOL using MATLAB (middleware).

Fig. 4 depicts available coupling schemes associated with building energy and subsurface numerical software. Most subsurface tools, except for MATLAB and Fluent which can both function as FMU, have limited or no built-in coupling options, while there are various choices for coupling building energy tools. Specifically, Modelica, the building simulation tool with the highest coupling capability, can only be linked to four subsurface numerical tools.

4. Current research and modeling development

This section provides a comprehensive overview on co-simulation studies in the literature, focusing on case studies, energy systems and research trends.

To identify relevant co-simulation studies, a literature review was conducted in Scopus database using three search strings as follows:

- *Building energy* (TITLE–ABS–KEY: “building*” OR “office*” OR “house*” OR “district heating” OR “district cooling” OR “HVAC*”) AND
- *Geothermal systems* (TITLE–ABS–KEY: “ground heat exchanger*” OR “borehole heat exchanger*” OR “energy pile*” OR “foundation pile*”

Table 2
Feature comparison of common numerical software for geothermal systems. The following subsurface processes are considered: thermal (T), hydraulic (H), mechanical (M) and chemical (C).

Software	User interference		License		Numerical solver			Subsurface processes			
	CLI	GUI	Commercial	Open-source	FDM	FVM	FEM	T	H	M	C
Ansys Fluent [122]	○	●	●	○	○	●	○	●	●	●	○
COMSOL [123]	○	●	●	○	○	○	●	●	●	●	●
FEFLOW [124]	○	●	●	○	○	○	●	●	●	○	●
MRST [125]	○	●	○	●	●	●	●	●	●	●	●
OGS[a] [126]	●	○	○	●	○	○	●	●	●	●	●
MODFLOW[b] [127]	○	●	○	●	●	○	○	●	●	○	●
TOUGH [128]	●	○	●	○	○	●	○	●	●	○	○

[a] DataExplorer program is developed to provide a GUI for OGS.
[b] Including MT3DMS and SEAWAT models.

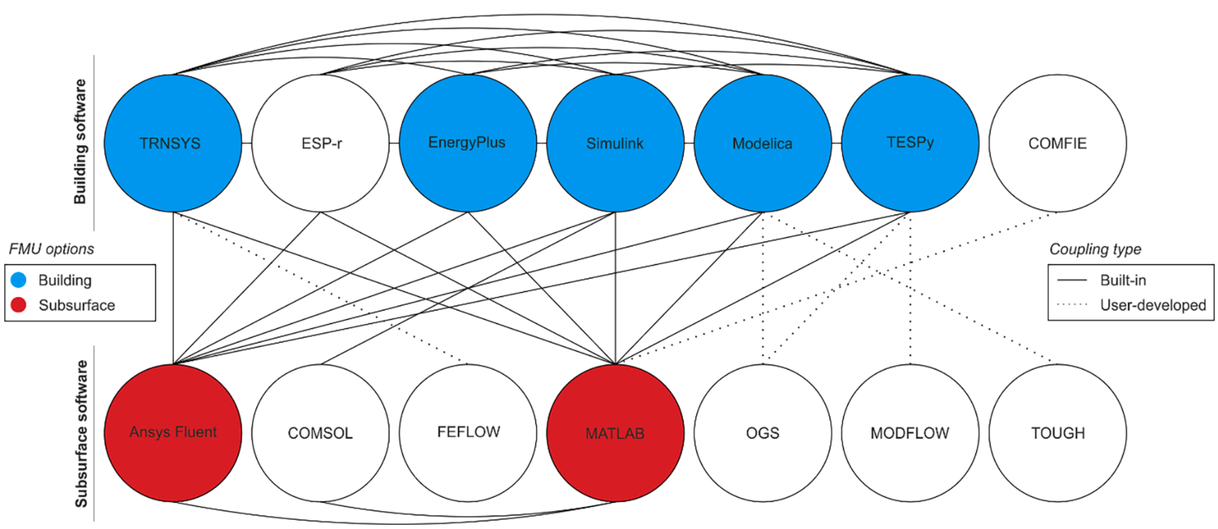

Fig. 4. Available software coupling options for co-simulation in the field of building energy and geothermal systems.

OR “borehole thermal energy storage” OR “aquifer thermal energy storage” OR “ground source heat pump*” OR “ground water heat pump*” OR “ground* heat pump” OR “geothermal heat pump*”) AND

- *Co-simulation* (ALL: “co-simulation” OR “cosimulation” OR “functional mock-up” OR (“coupl*” AND “simulat*”))

The last search was updated in March 2025 without any filtering on publication year and language. Scopus search results were then examined in detail to only include studies that have carried out co-simulation (as defined in Section 3).

4.1. Co-simulation case studies

A total of 141 co-simulation research articles were identified, presenting 242 case studies. Fig. 5 visualizes the global distribution of these case studies. Co-simulation of geothermal systems and building energy was mostly conducted in Europe (47 %), the USA (23 %) and China (11 %), while the rest of the world accounts for less than 20 %. Studies focused on BHE (65 %), followed by BTES (19 %), GHE (8 %), ATES (3 %) and EP (2 %). Hybrid geothermal systems such as GHE + BHE, GHE + BTES and BHE + BTES, alongside GWHP, each contribute to less than 1 % of the research. Over two-thirds of BTES studies were conducted in Europe and China, while EP was only investigated in USA [138] and Canada [139]. Co-simulation of open geothermal systems was examined exclusively in European countries: ATES in Germany [140,141] and the Netherlands [142,143], and GWHP in Italy [144]. Moreover, hybrid geothermal systems are solely investigated in USA [145], China [47], Italy [146,147] and Norway [148].

Fig. 6 summarizes the application of co-simulation studies in the building energy sector. Over 80 % of the studies focused on individual residential, commercial and institutional buildings, while only 19 studies (8 %) were performed on district scale (only with closed geothermal systems). Some studies analyzed other building types including the German Parliament [140], a historical library [149], data centers [141], multi-purpose/load sharing buildings [150,151], an earth shelter [152] and a municipal building [74]. Geothermal systems are mainly used for heating & cooling (73 %), followed by heating-only (21 %) and cooling-only (6 %) applications, indicating little co-simulation research in warm, cooling-dominated regions.

4.2. Energy systems analysis in co-simulation

Fig. 7 outlines hybrid geothermal-based energy systems examined in co-simulation studies so far. Moreover, the exact system configurations for all case studies are provided in Appendix B. Integrating shallow geothermal systems with GHP was the most common approach [139,142,153,154]. The performance of BHE was extensively investigated with a variety of energy components, such as dual (air + ground) source HP (DSHP) [155–158], district heating [93,159], PCM [74,160] and hybrid renewable energy systems [161,162].

Most BTES studies involved thermally recharging of BHE using solar technologies, also known as solar assisted GSHP (SAGSHP) [163–169], or waste heat sources [170,171] to alleviate ground temperature drops. Also, BTES was modeled using two independent BHE fields for seasonal energy storage [10]. In addition to BHE, EP-based geothermal systems were recently considered for modeling BTES [172,173]. Open geothermal systems have so far only been integrated with few types of

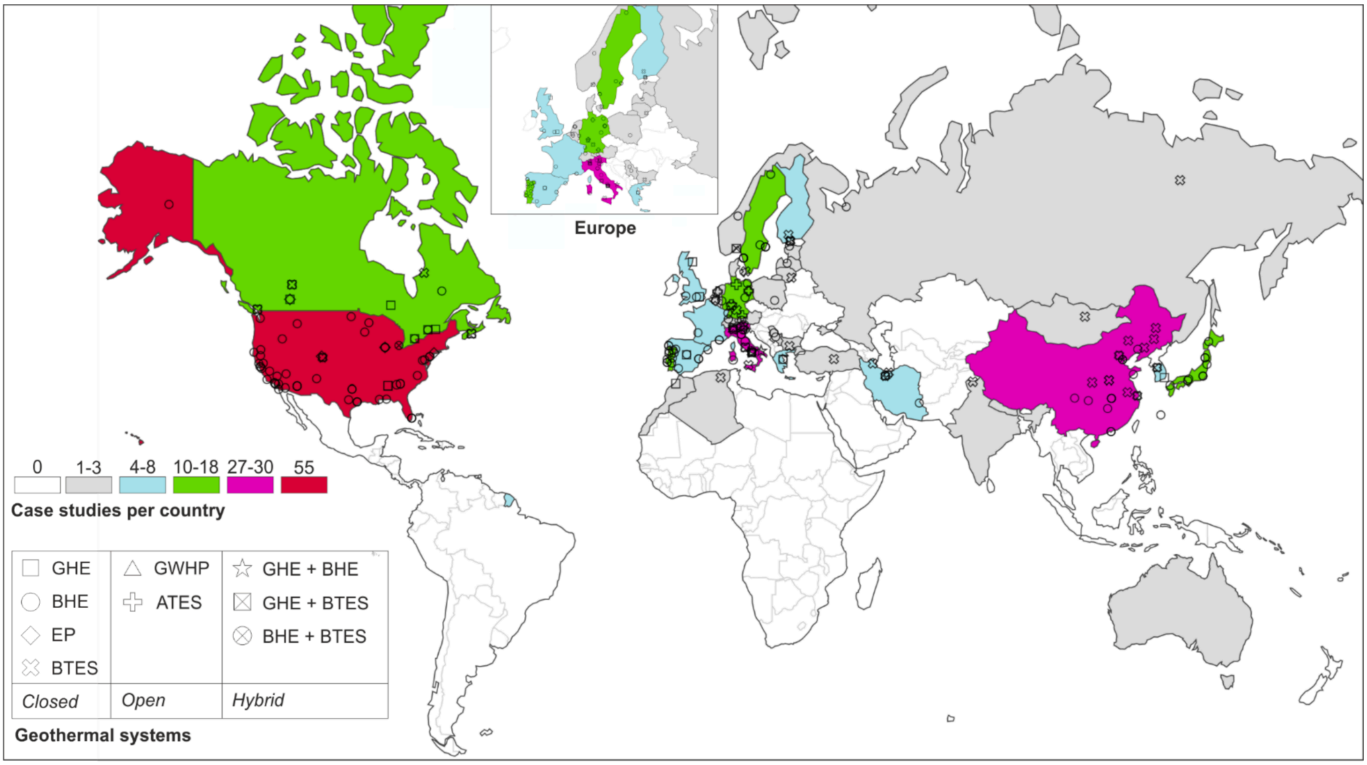

Fig. 5. Spatial distribution of co-simulation research for various geothermal systems.

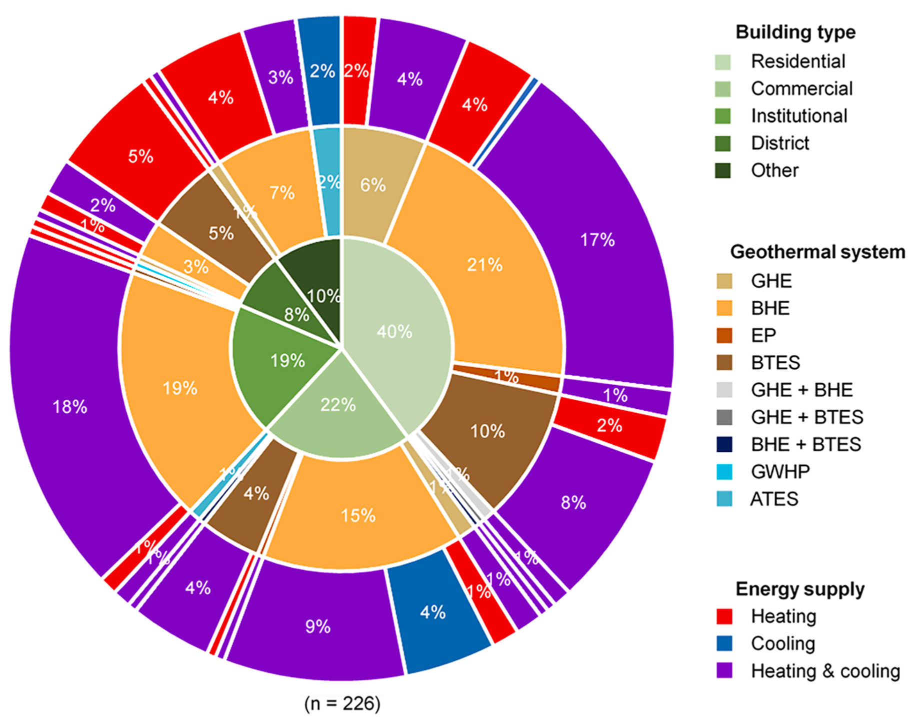

Fig. 6. Classification of co-simulation studies by buildings, geothermal systems and energy supply. Heating includes space and/or water heating supply.

thermal energy systems including GHP [142,143], STC [144], chiller [140] and cooling tower [141]. It is worth noting that most EP and BTES studies also modeled a typical BHE case for comparison [138,139,161,163,164,166,174].

Fig. 8 gives an overview on the different performance indicators commonly applied in co-simulation studies. Techno-economic and environmental results of co-simulation studies show a system COP of 4 ± 1, discomfort time of 6 % ± 4 %, payback period of 14 ± 9 years and annual CO_2 emission savings of 40 % ± 27 %. This implies a wide range of system performance, especially for economic and environmental metrics, emphasizing that the efficiency and attractiveness of geothermal systems are highly dependent on system characteristics and climatic conditions. A distinction of geothermal systems performance is

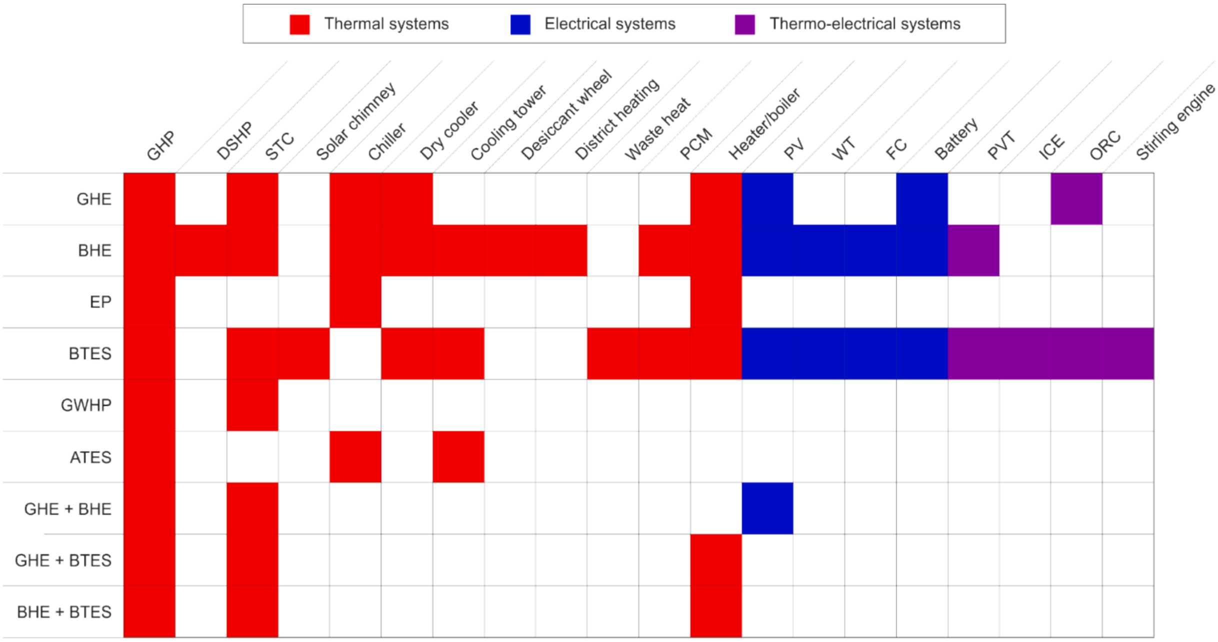

Fig. 7. Integration of geothermal systems with thermal, electrical and thermo-electrical technologies in co-simulation studies.

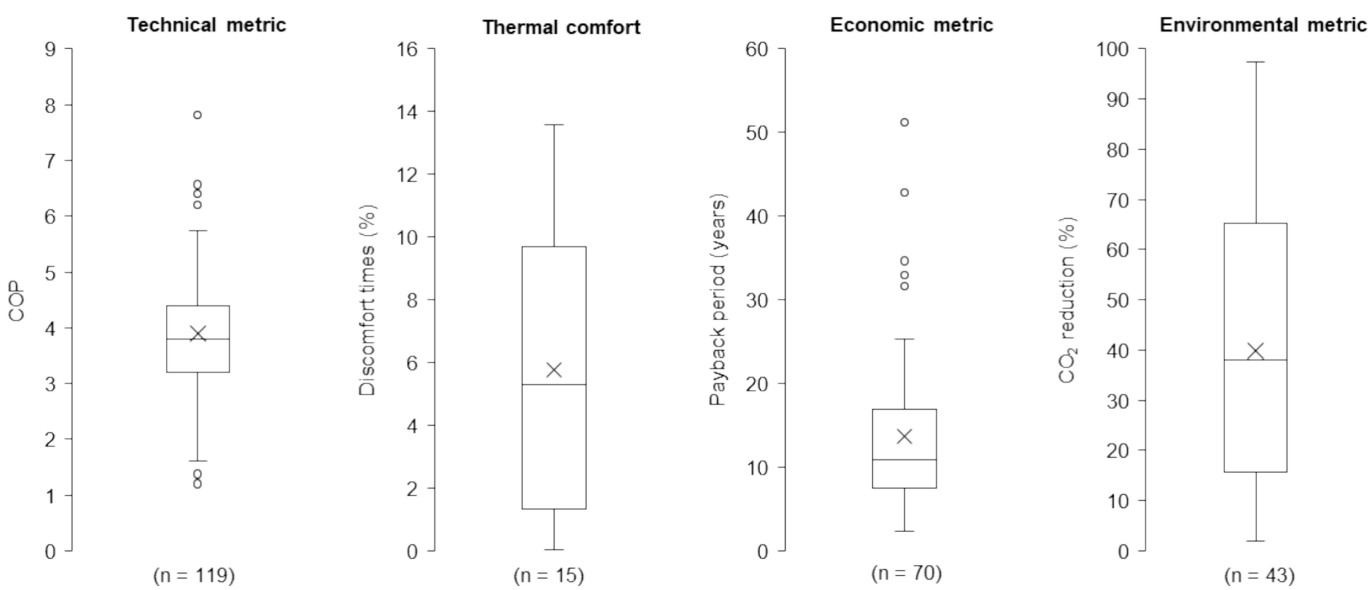

Fig. 8. Technical, thermal comfort, economic and environmental results of co-simulation studies. The cross and circle symbols represent the mean values and outliers, respectively.

not provided, as it could lead to incorrect conclusions for technology comparison due to operation under different systems and climates.

It is also important to note that only a few studies conducted thermal comfort assessment for heating and cooling of buildings using geothermal systems, either by simply analyzing unmet hours when the indoor temperature is outside the set-point comfort range [150,163,175–177] or by applying the standard Fanger's PMV-PPD model [147,178–180]. This implies that indoor comfort condition is currently not the main focus of the application of co-simulation.

4.3. Research trends in co-simulation

Fig. 9 summarizes the progress of co-simulation in literature, from initial feasibility studies to advanced research, categorized into four phases:

First phase (2005–2010)

The first phase involves few simplified feasibility studies on basic geothermal systems including GHE, BHE and GWHP with traditional building energy tools. For instance, eQUEST and VisualDOE (DOE-2 based tools) were employed for modeling and performance analysis of BHE and GWHP, respectively [144,181]. In this period, only one optimization study was found for a limited design space by incorporating co-simulation in TRNSYS [182].

Second phase (2010–2015)

In the second phase, approaches became more detailed for specific geothermal cases. Montagud et al. [183] developed a valid TRNSYS model for a real GSHP system installed in a university office building.

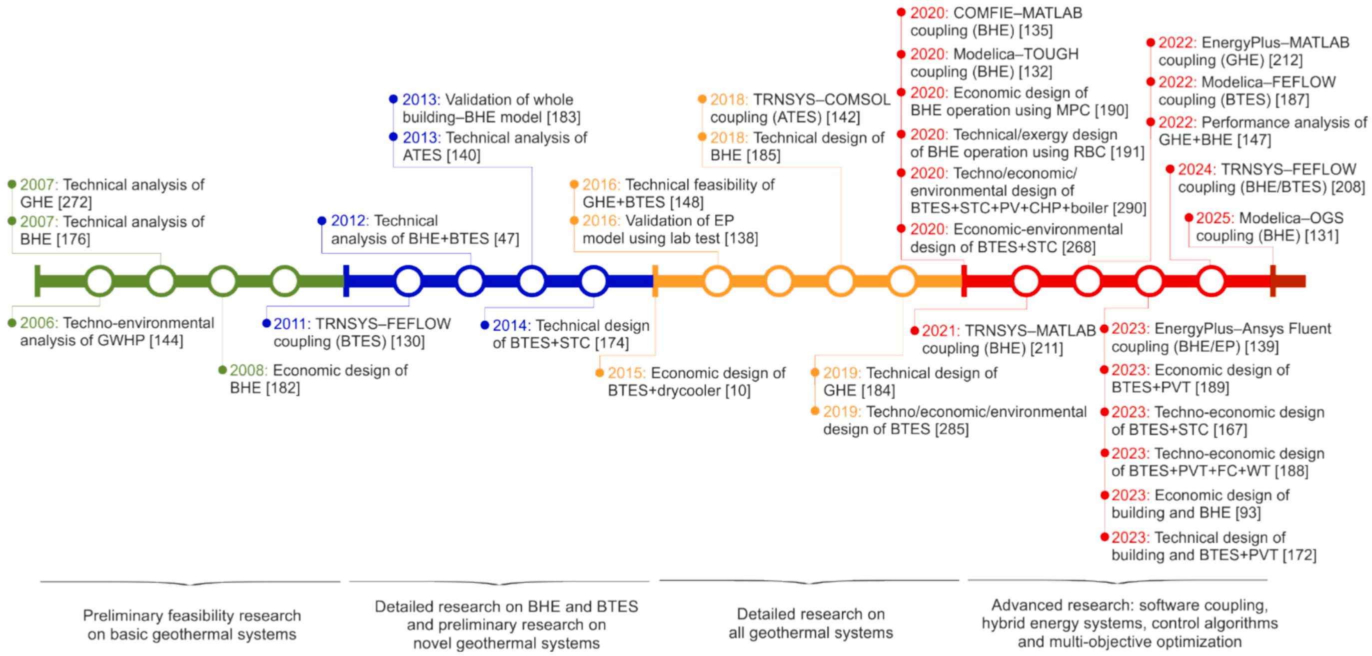

Fig. 9. Research focus of co-simulation studies in the literature.

Diersch et al. [130] coupled TRNSYS with FEFLOW for fully discretized 3D modeling of a BTES system in a co-simulation study. Another design study was identified for finding optimal configuration of a hybrid BTES + STC system based on a few TRNSYS co-simulation runs. In a novel study, Wang et al. [47] analyzed a hybrid system consisting of both BHE and BTES to supply cooling and heating loads, respectively. Additionally, a simplified technical analysis on ATES emerged using TRNSYS [140].

Third phase (2015–2020)

The third stage covers co-simulation for various geothermal technologies in greater detail. For instance, Kwag & Krarti [138] implemented a validated EP model for co-simulation in EnergyPlus. Also, Bozkaya et al. [142] linked TRNSYS with numerical model of ATES in COMSOL. Nord et al. [148] analyzed the feasibility of BTES with a GHE-based ventilation system. Moreover, few design studies were conducted for GHE [184], BHE [185] and BTES [10,165], primarily in TRNSYS and EnergyPlus.

Fourth phase (2020–2025)

Since 2020, research has progressed to an advanced level. Specifically, various building and subsurface tools are coupled for more accurate system analysis with multiple software co-simulation [131,186,187]. Many hybrid geothermal-based energy systems are analyzed and designed using single- and multi-objective optimization [188,189]. For instance, Ferrara & Fabrizio [167] used GenOpt optimization toolbox for multi-objective design of a SAGSHP system developed in TRNSYS using global cost and seasonal performance factor. Some research also focused on optimizing control strategies for the application of geothermal systems in buildings [190–192]. Recently, Hermans et al. [193] showed that MPC results in up to 17 % cost reductions for a district-scale GSHP compared to traditional RBC. Appendix C contains a comprehensive presentation of all optimization studies with main findings.

5. Software and model usage

A variety of software tools and geothermal models are used in the literature for conducting co-simulations (Appendix D). TRNSYS has been the primary software for performing co-simulation of building-integrated geothermal systems (58 %). Studies predominantly applied the duct ground heat storage (DST) model for BHE and BTES simulations. However, due to the modeling limitations of DST, some research developed new modules [194–196] or combined multiple components to simulate a single geothermal system. For instance, DST model was integrated with a heat exchanger component (Type 997) to simulate the underground pipes connecting the BHE with the GHP [197]. Also, Allaerts et al. [10] incorporated both DST and EWS (a transient BHE model) modules to simulate cold and warm borefields of a BTES system, respectively.

Co-simulation studies with other whole-building tools, except for IDA ICE, have mostly adopted *g*-function based techniques (thermal response factors) for BHE and BTES modeling. IDA ICE, however, contains FDM models for interacting boreholes [173,198], as well as a simplified GHE model assuming a constant or scheduled ground temperature for heat collection and disposal [148]. It is worth mentioning that software often employ various response factors: steady-state long-term *g*-function (LTG) [185,199], enhanced LTG by extrapolation of *g*-functions to shorter times accounting for transient effects [200,201], as well as combination of LTG with short-term *g*-function (STG) [152,175] (see Appendix A). Different approaches are available for determination of STG and LTG [202–205].

16 studies conducted co-simulation using multiple software (11 %), mainly for employing a high-fidelity subsurface model [130,131,186]. However, some studies coupled multiple software to develop advanced controllers [206]. For instance, Cucca & Ianakiev [207] imported building energy model developed in EnergyPlus into Modelica (Dymola) as a FMU to test various control logics for the energy system

Fig. 10 summarizes physical mechanisms accounted for modeling closed geothermal systems in co-simulation studies using single and multiple software. Single software approaches were solely based on heat transport modeling in the subsurface, considering the effects of axial heat flux (91 %), thermal interaction (90 %) and geothermal mass for transient response (26 %). However, software coupling facilitated

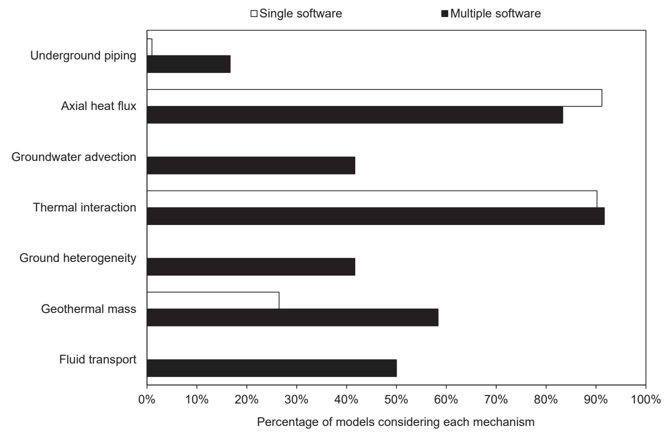

Fig. 10. Summary of subsurface modeling fidelity for closed geothermal systems in co-simulation studies with single and multiple software.

detailed physics subsurface simulation by modeling fluid transport [130,131,142,143,186,187,208,209], ground heterogeneity [130,131,186,208,209] and groundwater advection [130,131,186,187,208]. Only a very few studies modeled underground hydronic circuits of geothermal systems in co-simulation studies [187,197,208]. This could affect the validity of subsurface models by ignoring underground heat losses, especially in large geothermal systems with complex series and parallel piping networks.

Existing co-simulation research on open systems are based on subsurface models with significant simplifying assumptions. Specifically, Ferrari et al. [144] modeled a GWHP with a constant predefined groundwater temperature. Also, current ATES studies adopted 2D axisymmetric models with thermo-hydraulically independent wells [140–143].

6. Challenges of co-simulation

This section presents current challenges in the field of co-simulation with a focus on computational issues of software coupling, as well as results validation.

6.1. Computational and software coupling issues

Fig. 11 shows coupling approaches adopted in co-simulation studies using multiple software. Coupling is primarily conducted using text files [132,143,209], which is also the most error-prone and time-consuming method, followed by network connections [130,131,210] and embedded functions [206,207]. For instance, Bozkaya et al. [142] exchanged input/output data between TRNSYS and COMSOL during co-simulation using a common database with text files. Adebayo et al. [139] developed a user defined function (UDF) in Ansys Fluent to create a coupling interface with EnergyPlus. Diersch et al. [130] established RPC connection between TRNSYS and FEFLOW, while Randow et al. [131] linked Modelica with OGS through TCP/IP. Alaie et al. [211] imported the MATLAB code of a BHE model into TRNSYS using Type 155 as an embedded function. Similarly, Kharbouch et al. [212] used BCVTB platform to exchange data between EnergyPlus and MATLAB during co-simulation.

Notably, no research so far employed parallel synchronization; only one used iterative synchronization [135], while the remaining studies applied non-iterative sequential synchronization (Fig. 3c). Furthermore, Modelica and TRNSYS have not been coupled with any subsurface tool using FMI standard, highlighting the limited number of subsurface tools currently offering FMU option. Some robust subsurface tools like MODFLOW and MRST have not been used for co-simulation despite available coupling options (see Table 2 and Fig. 4). This emphasizes the sophistication involved in establishing a coupling scheme between software tools.

Table 3 reports the run-time and transmission error of co-simulation studies. Annual simulation is carried out within half an hour for semi-analytical geothermal models [132,135], but can take over 4 h for high-fidelity, fully discretized models [131]. Transmission errors in software coupling ranged from 0.2 % to 26 %, depending on the communication (macro) time step. Clearly, a short communication length reduces data transmission errors, but on the other hand, it leads to longer simulation times by requiring more subsurface solves. These transmission errors and computation times can impede the extensive use of detailed co-simulation with multiple software for model validation and system design purposes.

6.2. Validation in co-simulation

Validation involves assessing the model's accuracy by comparing simulation results with actual data to determine how well the model represents the real-world system. Validation can be performed graphically or with statistical methods. Graphical methods identify where simulation outputs differ from measured values, but they are not able to quantify the error as basis for comparison of different simulation results.

Statistical methods, on the other side, can be applied for error quantification. Mean relative error (MRE), mean bias error (MBE), root mean square error (RMSE) and coefficient of variation of root mean square error (CV(RMSE)), are common error metrics for validation

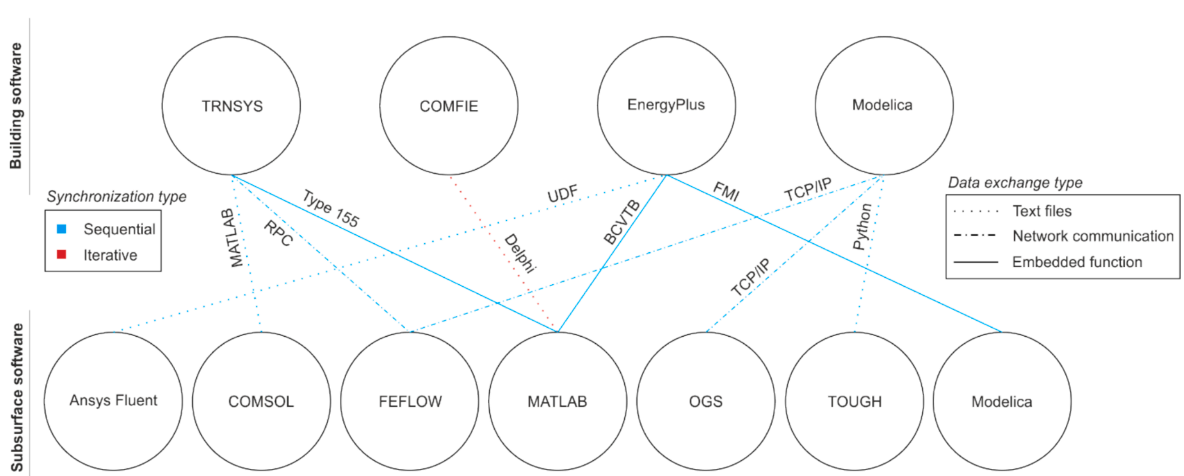

Fig. 11. Adopted coupling approaches in existing studies for co-simulation of building energy and geothermal systems.

Table 3
Reported simulation time and error in co-simulation studies with software coupling.

Software	Model type	Geothermal system	Communication time step (h)	Yearly simulation time (min)	Transmission error (%)	Reference
COMFIE-MATLAB	LTG	26 × 26 BHE	0.5	8	N/A	[135]
Modelica	HSRM[a]	Single BHE	1	19	N/A	[132]
Modelica-TOUGH	2D FVM			23		
Modelica-FEFLOW	MoBTES	18 BHE	2.2[b]	40	2.0–26.2[c]	[187]
	3D FEM			156		
Modelica-OGS	3D FEM	3 BHE	1	282	0.17	[131]
			6	60	0.23	
			12	36	0.48	
			24	24	6.49	

[a] Semi-analytical built-in Modelica package for BHE modeling, as described in Appendix A.
[b] Average value for different cases changing communication time step from 2 min to 1 day.
[c] Depending on the coupling variable and strategies for system operation and communication time step control.

purposes, defined in Eq. (10)–(13), respectively:

$$MRE = \frac{\sum_{i=1}^{n}(s_i - m_i)/m_i}{n}, \quad (10)$$

$$MBE = \frac{\sum_{i=1}^{n}(s_i - m_i)}{\sum_{i=1}^{n} m_i}, \quad (11)$$

$$RMSE = \sqrt{\frac{\sum_{i=1}^{n}(s_i - m_i)^2}{n}}, \quad (12)$$

$$CV(RMSE) = \frac{RMSE}{\overline{m}}, \overline{m} = \frac{\sum_{i=1}^{n} m_i}{n}, \quad (13)$$

where n is the number of data points used, and m_i and s_i refer to measured and simulated data, respectively.

MRE and MBE report actual data discrepancy, but they can be misleading because positive and negative errors may cancel each other out (offsetting error). On the other hand, RMSE shows the spread or variability of discrepancy without an offsetting error by summing the squared differences. Moreover, CV(RMSE) gives a relative measure of error for clearer comparison of different scenarios by normalizing RMSE based on mean of observed data. Combining graphical methods with quantitative error metrics can highlight the points where errors exist, as well as their direction and magnitude.

There are several standards for model validation. ASHRAE Guideline 14–2014 [213] and International Performance Measurements and Verification Protocol (IPMVP) [214] are widely used in the literature for validation of the whole-building model. Overall, IPMVP sets stricter thresholds compared to ASHRAE, especially for data with an hourly sampling period (Table 4).

Fig. 12 presents the results of validation efforts in co-simulation research using experimental data. A few studies validated their models (< 10 %), which were limited to closed systems. All models were reported to be well calibrated based on the abovementioned criteria. On average, validation studies reported MBE as 4 % ± 2 %, RMSE as 1 °C ± 0.2 °C and CV(RMSE) as 10 % ± 5 %. However, validation is focused on the whole building–geothermal model, by analyzing indoor temperature [168,215] or energy consumption [146,216]. Also, graphical error analysis showed that significant differences between measured and simulated data could occur, mainly because of using steady-state geothermal models [168]. For instance, Cho & Mirianhosseinabadi observed up to 600 kWh discrepancy between measured and simulated monthly electricity consumption [217]. Therefore, great care should be taken when using simplified semi-analytical models for geothermal-based system design [182].

Table 4
Thresholds of different protocols for model validation using hourly and monthly data.

Standard	CVRSME (%)		MBE (%)	
	Hourly	Monthly	Hourly	Monthly
ASHRAE Guideline 14	±30	±15	±10	±5
IPMVP	±20	±15	±5	±2

7. Conclusions and outlook

This review presented the current status of co-simulation between building energy and geothermal systems, highlighting modeling approaches, coupling methods, software tools, as well as their application in case studies. Considering the increasing interest in the field, it is crucial to address the following research gaps and areas for improvement to strengthen co-simulation in future studies:

Geothermal systems

Two-thirds of co-simulations focused on BHE systems, while less than 5 % investigated energy piles and ATES, despite their high efficiency. This is because building energy tools lack built-in packages for modeling such sophisticated systems. Hence, it is imperative to develop libraries for modeling these efficient geothermal systems, especially in Modelica, due to its modular environment and capabilities for designing real-world controllers and district-scale simulations.

Software coupling

Although many tools are available for detailed co-simulation through software coupling, only 10 % of studies conducted co-simulation using multiple software. This could be due to a lack of knowledge about existing tools, as well as the complexity of coupling schemes. This study explored various techniques for software coupling, including simple data exchange methods by reading and writing text files during co-simulation, which can be easily implemented in the corresponding software by developing user objects.

Long run-time along with transmission errors are currently the main challenges for co-simulation with software coupling. Therefore, improved coupling algorithms (synchronization schemes) and software options should be devised to reduce these computational issues. Such optimized approaches can then be applied to advance co-simulation case studies, which will enable reliable performance analysis of geothermal systems in building energy applications.

Model validation

Most validation studies adopted an all-encompassing calibration approach for the entire system by applying semi-analytical geothermal models in whole-building tools. Such models should only be used for initial feasibility studies. A step-by-step validation approach (i.e., starting with the subsurface, followed by the building, and then the entire system) is a prerequisite for developing an accurate model for

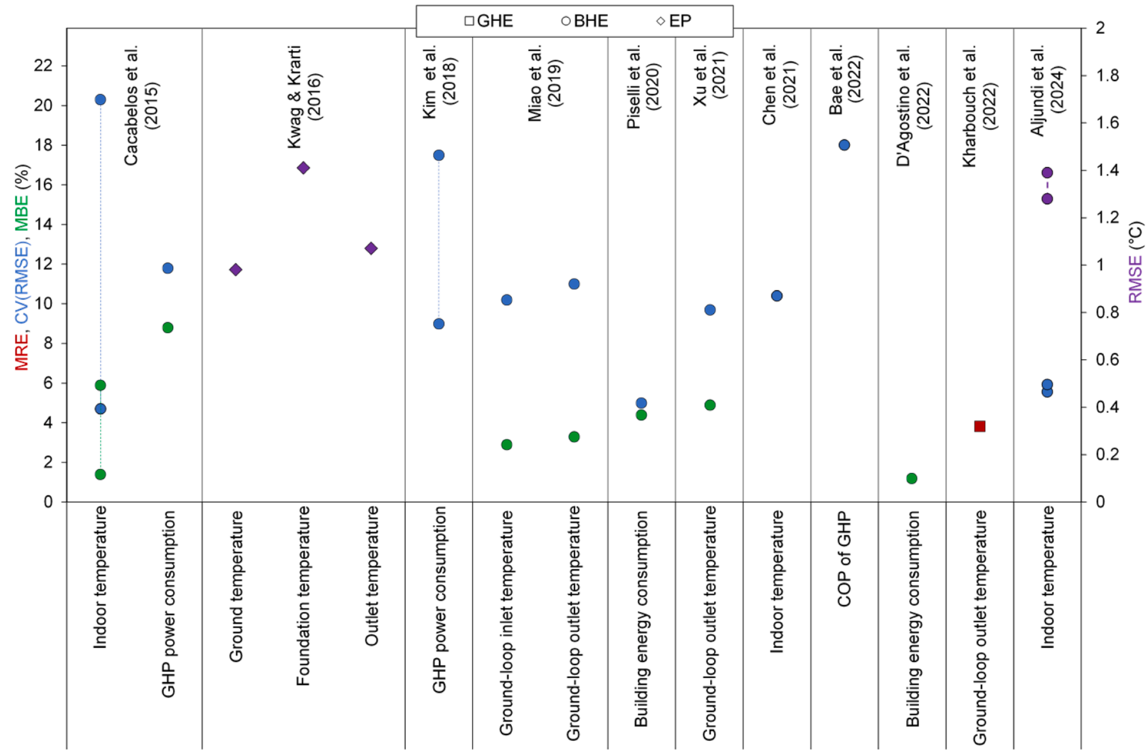

Fig. 12. Results of experimental validation for building integrated geothermal models in co-simulation studies. Error metrics variations for indoor temperature and GHP power consumption are due to different building zones and seasons, respectively. Absolute values of MBE are considered.

design purposes.

There are different standards for subsurface model validation, which could be employed in calibration efforts [218]. For instance, the German Water and Gas Association (DVGW) provides guidelines for groundwater model calibration [219].

This however requires models with detailed representation of the subsurface. This can be done by coupling building energy software with a subsurface numerical tool or implementing more accurate semi-analytical geothermal models in whole-building tools. For instance, thermo-hydraulic modeling of underground distribution networks of geothermal systems can be done by coupling OGS with TESPy [220]. Also, there are high-fidelity semi-analytical models, such as moving finite line source (MFLS), accounting for both groundwater advection and ground surface effects, which can be incorporated in whole-building tools for fast subsurface model validation [221,222].

Optimization

Geothermal systems are often designed based on a separate simulation approach by specific design tools such as GLHEPro and EED incorporating thermal loads obtained from a building energy software. Such decoupled approaches cannot ensure indoor thermal comfort and are not capable of operation optimization or hybrid geothermal-based system design.

20 optimization studies based on a co-simulation approach were identified. However, because of high computational costs and lack of optimization modules, most studies considered a very limited design space, linked whole-building software with optimization tools such as GenOpt and MOBO, or used statistical and machine learning methods for system optimization based on outputs of a few co-simulation runs.

In this regard, developing a platform-based design (PBD) framework [223] for the optimization of geothermal-based systems, considering a co-simulation approach, is of decisive importance. Such a framework can facilitate the integration of optimal geothermal systems into buildings across various types and scales.

CRediT authorship contribution statement

Hamed Yazdani: Writing – review & editing, Writing – original draft, Software, Methodology, Investigation, Formal analysis, Conceptualization. **Philipp Blum:** Writing – review & editing, Writing – original draft, Supervision, Resources, Project administration, Methodology, Investigation, Funding acquisition, Formal analysis, Conceptualization. **Kathrin Menberg:** Writing – review & editing, Writing – original draft, Supervision, Resources, Project administration, Methodology, Investigation, Funding acquisition, Formal analysis, Conceptualization.

Declaration of competing interest

The authors declare that they have no known competing financial interests or personal relationships that could have appeared to influence the work reported in this paper.

Acknowledgements

This work was supported by the German Federal Ministry for Economic Affairs and Energy [grant number FZK 03EE4040] in the context of the GEOTHERMICA & JPP SES Joint Call 2021 “Accelerating the Heating & Cooling Transition”. The research was conducted as part of the Geothermal-based Optimized Energy Systems (GOES) project.

Appendix

A. Summary of available components and modules in building energy software for simulation of geothermal systems along with a brief description. Abbreviations: conduction transfer function (CTF), duct ground heat storage (DST), finite cylindrical source (FCS), hybrid step response model (HSRM), infinite line source (ILS), long-term g-function (LTG), thermal resistance model (TRM) and thermal resistance–capacitance model (TRCM).

Geothermal system	Software	Component/library	Model	Note	Ref
GHE	TRNSYS	Type 997[a]	FDM	- straight tubes with variety of flow configurations (parallel, counter flow, serpentine, etc.) - shallow trenches with evenly spaced identical pipes - modeling variable ground surface boundary, building interaction and distinct soil layers	[224]
		Type 460[b]	Hypocaust	- straight tubes - air-to-soil GHE - modeling latent and sensible heat exchange inside the tube, diffusion in soil, internal pressure drop and condensed water flow using analytical formulae	[225]
		Type 556[b]	TRM	- straight tubes - 2D symmetric model considering conduction in the radial and circumferential directions	[196]
	EnergyPlus	GroundHeatExchanger: Surface	Modified CTF	- straight tubes - fast/simplified model for simulating heat rejection using hydronic tubes located at very shallow depths (< 1 m)	[226]
		Pipe:Underground	FDM	- straight tubes with parallel flow - 2D rectangular conduction model with axisymmetric heat transfer near pipes	[226]
		PipingSystem: Underground[c]	FVM	- straight tubes with different flow configurations and trench layouts - detailed fully 3D model with dual coordinate system - allowing mesh modification, variable surface boundary conditions and building interaction	[226]
		GroundHeatExchanger: Slinky	LTG	- horizontal and vertical slinky tubes with uniform length, equidistant and single layer trenches - modeling slinky tubes as multiple detached rings with *g*-function technique	[226]
	DOE-2	HORIZ-STRAIGHT-LOOP	TRM	- straight tubes with 6 pre-set tube configurations (single, two- and four- pipe with series and parallel flow) - modeling soil temperature by superposition of undisturbed soil temperature (transient cosine function of depth and soil properties) and a sink/source term due to heat pulses imposed by GHE	[227]
		HORIZ-SLINKY-LOOP	TRM	- horizontal and vertical slinky tubes with multiple parallel trenches in a single ground layer - modeling slinky tubes with equivalent U-bend heat exchanger	[227,228]
	ESP-r	H4, HS, SL	ILS	- straight and slinky tubes with three configurations (two pipe in single layer, two pipe in two layer and horizontal slinky) - modeling based on ILS with daily calculation	[111]
BHE	TRNSYS	Type 557[a, d]	DST	- U-tube BHE with uniform distribution within a cylindrical storage duct - steady-state model based on the superposition of solutions for local (near boreholes) and global (ground storage and losses) heat transfer processes - only one borehole field per model	[229]
		Type 257[b]	Enhanced DST	- modified DST code allowing to model two independent borefields	[230,231]
		Type 281[b]	LTG	- U-tube BHE with arbitrary distribution - steady-state model based on the classical Eskilson's LTG	[232]
		Type 451[b]	EWS	- single U-tube BHE - transient model based on TRCM and ILS	[233]
	EnergyPlus	GroundHeatExchanger: Vertical	LTG + STG[e]	- U-tube BHE with arbitrary distribution - transient model based on long- and short-term *g*-function	[226,234]
	Modelica	UTube	TRCM + CTF	- single U-tube BHE - transient model based on TRCM and CTF	[235,236]
		HSRM	TRCM + LTG	- U-tube BHE with parallel distribution - transient model based on TRCM and long-term *g*-function (based on uniform heat flux approach)	[235,237]
		gFunction	FCS + ILS + LTG	- U-tube BHE with arbitrary distribution - transient model by combining long-term g-functions with finite cylindrical- and infinite line source solutions	[238–240]
		MoBTES	Modified DST	- U-tube BHE with arbitrary distribution - integrating equivalent radii approach and TRCM into DST approach	[241]
	IDA ICE	Boreholes[d]	FDM	- U-tube BHE with arbitrary distribution - transient model based on 1D heat transfer within and 2D heat conduction outside BHE	[242,243]
	DOE-2	VERT-WELL-FIELD	LTG	- U-tube BHE with predefined configurations (single, line, L-shaped, U-shaped and rectangle) - steady-state model based on the classical Eskilson's LTG	[227,244]
		VERT-WELL-NEW	Enhanced LTG	- U-tube BHE with available configuration (single, line, L-shaped, U-shaped and rectangle) - transient model based on modified Eskilson's LTG (linear extrapolation of *g*-functions to shorter times)	[227,244]
	ESP-r	V1	ILS	- single U-tube BHE - transient model based on the ILS with daily calculation	[111]
EP	TRNSYS	Type 80[b]	TRNVDSTP	- U-tube BHE with uniform distribution within a cylindrical storage duct	[245]

(continued on next page)

(*continued*)

Geothermal system	Software	Component/library	Model	Note	Ref
ATES	TRNSYS	Type 345[b]	TRNAST	- modified DST by accounting for different ground layers, groundwater flow and piping over the ground surface - two-well ATES - 2D axisymmetric model for thermally and hydraulically independent wells without groundwater flow	[246]

[a] In new TRNSYS TESS library v18, Types 548 and 999 were introduced to allow modeling multiple fields/instances of GHE and BHE, respectively, per project.
[b] Non-standard/user written components.
[c] The object GroundHeatExchanger:HorizontalTrench inherits the model of PipingSystem:Underground with simpler inputs by sacrificing several features such as mesh refinement and modeling trenches with different depth and distance.
[d] Able to model EP by changing ground boundary conditions.
[e] Depending on the user input for *g*-functions, boreholes may be modeled by only LTG.

B. Geothermal-based systems investigated in co-simulation studies. Abbreviations: dual source heat pump (DSHP), electric heat pump (EHP), fuel cell (FC), geothermal heat pump (GHP), heat pump (HP), internal combustion engine (ICE), organic Rankine cycle (ORC), phase change material (PCM), photovoltaic (PV), photovoltaic thermal (PVT), solar thermal collector (STC), Stirling engine (SE) and wind turbine (WT).

GHE	BHE	EP	BTES	GWHP	ATES	GHE + BHE	GHE + BTES	BHE + BTES
Stand-alone [212,247]	Stand-alone [94,248–250]	GHP [139]	GHP [173]	GHP + STC [144]	GHP [142,143]	GHP + dedicated HP [146]	GHP + STC + boiler [148]	GHP + STC [47]
GHP [153,251]	GHP [135,149,154,175,176,180–183,185,191,193,195,197,198,200,211,215–217,252–265]	GHP + chiller + boiler + DHW heater [138]	GHP + STC [163–168,174,266–270]		GHP + cooling tower [141]	GHP + STC + PV [147]		GHP + STC + gas heater [145]
GHP + dry cooler [184,194]	DSHP [155–158]		GHP + dry cooler [10]		Chiller [140]			
GHP + PV [271,272]	GHP + EHP [150]		GHP + PVT [189,273]					
STC + biomass-fired heater + absorption chiller + ORC + battery [196]	GHP + STC [177,199,274–277]		GHP + ORC [171]					
	GHP + cooling tower [179,275]		GHP + thermal ideal source [190]					
	GHP + boiler [192]		GHP + solar chimney + PVT [278]					
	GHP + PCM tank [74,160,279]		GHP + STC + ORC [280]					
	GHP + dry cooler + district heating [93,159]		GHP + STC + PCM tank [169]					
	GHP + STC + desiccant wheel [281]		GHP + PVT + battery [172]					
	GHP + STC + chillers (vapor compression/absorption) + cooling tower + auxiliary heater[a] [282]		GHP + PV + PVT + boiler [283]					
	Chiller + cooling tower + dry cooler [206]		GHP + diesel furnace + PV + battery [208]					
	STC + chillers (vapor compression/absorption) + cooling tower + auxiliary heater[a] [284]		GHP + WT + FC + PVT + battery [188]					
	GHP + PV [152,178]		STC [130]					
	GHP + FC [151]		STC + boiler [285]					
	GHP + EHP + PV [286]		STC + industrial waste heat [170]					
	GHP + chiller + PV [287]		STC + boiler + ICE + SE[a] [288]					
	GHP + boiler + PV [289]		STC + boiler + PV + ICE + SE + battery[a] [290]					
	GHP + PV + battery [207,291,292]		STC + adsorption chiller + cooling tower + boiler + PV + battery [293]					

(*continued on next page*)

(*continued*)

GHE	BHE	EP	BTES	GWHP	ATES	GHE + BHE	GHE + BTES	BHE + BTES
	GHP + WT + battery [294] GHP + STC + PV + battery [161] GHP + STC + chiller + boiler + PV [295] GHP + PV + PVT + electric heater [162] GHP + PVT [151,276,296–298]							

[a] Various system configurations were compared.

C. List of co-simulation studies with optimization. Abbreviations: area (A), length (L), capacity (C), back-propagation neural network (BPNN), Box–Behnken design (BBD), direct ground cooling (DGC), genetic algorithm (GA), life cycle cost (LCC), net present value (NPV), not-considered (NC), not-known (N/A), response surface methodology (RSM), seasonal performance factor (SPF) and thermally activated building (TAB).

Software (optimization tool)	Year	Location	Building	Annual loads (MWh) Heating	Cooling	Geothermal system	Design variables	Objective functions	Optimal system/ remarks	Reference
TRNSYS	2008	Québec, Canada	Residential	7	4	BHE	System size	LCC	DST model: L_{BHE} = 80 m, C_{GHP} = 1 ton. EWS model: L_{BHE} = 40 m, C_{GHP} = 1 ton.	[182]
TRNSYS	2014	Beijing, China	Office	N/A	N/A	BTES	Size of BTES and STC, flow rates of load and source sides of GHP	COP	The optimal system had 180 m BTES and 10 m^2 STC. The optimal ratio of source to load side flow rate was around 1.5.	[174]
TRNSYS	2015	Helsinki, Finland	Residential	69	1	BTES	Size of BTES and size and configuration of STC	Energy consumption	The optimal system included 150.5 m BTES with 93.6 m^2 glazed flat plate collectors.	[165]
TRNSYS	2015	Flanders, Belgium	Office	29	69	BTES	Size of cold boreholes in a BTES and drycooler	LCC	The optimal system comprised 5 and 35 warm and cold boreholes, respectively, and a 11.4 kW drycooler.	[10]
EnergyPlus/ CaRM	2018	Padova, Italy	Office	~30	~50	BHE	Layout of borefield (L-shape, rectangular, U-shape)	COP	L- and U-shape layouts showed better thermal performance than the rectangular one.	[185]
TRNSYS	2019	Birmingham, USA New York City, USA Orlando, USA	Residential	N/A N/A N/A	N/A N/A N/A	GHE	Size of GHE	Energy consumption	L_{GHE} = 600 m L_{GHE} = 800 m L_{GHE} = 400 m	[184]
TRNSYS	2019	Naples, Italy	District	N/A	NC	BTES	Thermal conductivity of soil and grout, U-pipe spacing, heat carrier fluid type, BTES number and connection	Energy consumption/ CO_2 emission/ operation cost	6 series-connected BTES is the optimal system. Shank spacing and heat carrier fluid typology have not significant impact on overall performance.	[285]
Modelica	2020	Denver, USA	TAB	N/A	NC	BTES	MPC control inputs (GHP modulation signal, ground regenerator signal, auxiliary heater signal)	Operational cost	Pumping cost is reduced by 10 % thanks to optimal use of active regeneration based on long-term horizon prediction.	[190]
TRNSYS (BPNN and GA)	2020	Wuhan, China	Office	N/A	N/A	BHE	Load and source side GHP loops temperature	COP/exergy efficiency	Under optimal conditions, COP and exergy	[191]

(*continued on next page*)

(*continued*)

Software (optimization tool)	Year	Location	Building	Annual loads (MWh)		Geothermal system	Design variables	Objective functions	Optimal system/ remarks	Reference
				Heating	Cooling					
							differences, load side return water temperature, load side supply and source side return water temperatures and supply air temperature of AHU		efficiency of the system can be increased by 20.5 and 77 %, respectively.	
Modelica (TACO)	2020	Denver, USA	TAB	N/A	NC	BHE	COP model, MPC control inputs (GHP modulation signal, source fluid mass flow rate, boiler power)	Operational cost	A constant COP model results in abrupt on/off for GHP. Accurate prediction of COP can results in 3 % cost reduction.	[192]
TRNSYS	2020	Naples, Italy	District	N/A	NC	BTES	Configuration of plant including STC, PV, ICE, SE, NGB, WPB, BTES	Energy consumption/ CO_2 emission/ operation cost	The optimal configuration was STC + BTES + ICE for all single objective functions.	[290]
TRNSYS (MOBO)	2020	Lukla, Nepal	District	796	NC	BTES	Size of BTES and STC	LCC + cost of GHG emission	L_{BTES} = 2831–5959 m, A_{STC} = 516–521 m^2	[268]
		Dras, India		910					L_{BTES} = 3761–5973 m, A_{STC} = 648–652 m^2	
		Sivas, Turkey		419					L_{BTES} = 2138 m, A_{STC} = 286 m^2	
		Harbin, China		690					L_{BTES} = 3939 m, A_{STC} = 681 m^2	
		Ulaanbaatar, Mongolia		729					L_{BTES} = 3476–6000 m, A_{STC} = 680–693 m^2	
		Verkhoyansk, Russia		1166					L_{BTES} = 6000 m, A_{STC} = 1640 m^2	
IDA ICE	2022	Gothenburg, Sweden	Office	252-457[a]	81-469[a]	BHE	Size and layout of boreholes and plant configuration (DGC/GHP/DH)	BHE installation cost/land area	Borehole length is smaller for DGC + DH compared to DGC + GHP plant.	[159]
EnergyPlus	2022	16 locations in California, USA	Residential	477-3033[b]	0-2436[b]	BHE	Depth and number of boreholes	NPV	System including 16 BHE with 6.7 m depth was optimal in most regions.	[260]
TRNSYS (JEA)	2023	Jilin, China	Office	N/A	N/A	BTES	Size of BTES and PVT	LCC	L_{BTES} = 888 m, A_{STC} = 20 m^2	[189]
TRNSYS (GenOpt)	2023	Alps, Italy	Restaurant	119	NC	BTES	Number and depth of boreholes, size of STC and storage characteristics	LCC + SPF	Optimal design had 4 boreholes with depth of 350 m and about 36 m^2 STC. Optimal point was mainly specified by number of boreholes.	[167]
TRNSYS (RSM and BBD)	2023	Zhengzhou, China	Office	N/A	N/A	BTES	Size of BTES, PVT, WT and FC	Energy consumption + COP + LCC	System with 17 boreholes (1700 m), 132 m^2 PVT, 20 WT and 12 FC was optimal.	[188]
Modelica	2023	Belgium	District	N/A	NC	BHE	GHP size, controller type (MPC, RBC)	LCC	MPC can reduce GHP size by 10–17 % compared to RBC. District size and heterogeneity could have	[193]

(*continued on next page*)

(*continued*)

Software (optimization tool)	Year	Location	Building	Annual loads (MWh)		Geothermal system	Design variables	Objective functions	Optimal system/ remarks	Reference
				Heating	Cooling					
									conflicting impacts on the profitability of the MPC.	
IDA ICE	2023	Gothenburg, Sweden	Office	272-457[a]	81-469[a]	BHE	Building facade thermal parameters (walls U-value and windows G-values), plant configuration (GSHP + DGC or GSHP + DH)	LCC	DGC + GSHP system is more profitable for buildings with balanced thermal loads.	[93]
TRNSYS	2023	Shenyang, China	Office	188	60	BTES	Size of BTES, PVT installation angle, roof absorptivity	Energy performance metrics	The optimal building should have roof absorptivity of above 0.36, PVT tilt angle of 45° and as many as possible boreholes.	[172]

[a] Depending on the building external structure.
[b] Depending on the region.

D. Software and geothermal models used in co-simulation studies. Abbreviations: analytical (AN), borehole-to-ground (B2G), conduction transfer function (CTF), duct ground heat storage (DST), finite difference method (FDM), finite element method (FEM), finite volume method (FVM), g-function (g-func), infinite line source (ILS), quadratic transfer function (QTF), not-known (N/A), predefined temperature (PT) and thermal resistance capacitance model (TRCM).

Software	Geothermal system model						Reference
	GHE	BHE	EP	BTES	GWHP	ATES	
TRNSYS	3D FDM (Type 997)	–	–	–	–	–	[153,184]
	2D FDM (Type 556)	–	–	–	–	–	[196,251,271]
	AN (Type 460)	–	–	–	–	–	[247]
	3D FDM (Type 233)	–	–	–	–	–	[194]
	N/A	–	–	–	–	–	[299]
	–	DST (Type 557)	–	–	–	–	[149–151,154,157,160,162,178,179,183,191,252–259,274–277,279,281,286,291,292,294–298,300]
	–	DST (Type 557) + 3D FDM (Type 997)	–	–	–	–	[197]
	–	EWS	–	–	–	–	[182]
	–	FVM	–	–	–	–	[282]
	–	TRNVDSTP (Type 80)	–	–	–	–	[265]
	–	g-func (B2G)	–	–	–	–	[195]
	–	N/A	–	–	–	–	[156,180,284,301]
	–	DST (Type 557)	–	3D FDM (Type 997)	–	–	[145]
	–	DST (Type 557)	–	DST (Type 557)	–	–	[47]
	–	–	–	DST (Type 557)	–	–	[161,163–167,169,171,172,174,188,189,266–270,273,278,283,285,288,290,293]

(*continued on next page*)

(*continued*)

Software	Geothermal system model						Reference
	GHE	BHE	EP	BTES	GWHP	ATES	
	–	–	–	DST (Type 557) + EWS	–	–	[10]
	–	–	–	–	–	2D FDM (Type 345)	[140,141]
EnergyPlus	–	g-func	–	–	–	–	[74,152,155,185,199,215–217,260–262,287]
	–	–	g-func	–	–	–	[138]
IDA ICE	PT	–	–	2D FDM	–	–	[148]
	–	2D FDM	–	–	–	–	[93,94,159,177,198,248–250,263]
	–	–	–	2D FDM	–	–	[173]
Modelica	–	g-func	–	–	–	–	[192,193,289]
	–	–	–	g-func	–	–	[170,190,280]
	–	–	–	TRCM + CTF	–	–	[168]
DesignBuilder[a]	QTF	g-func	–	–	–	–	[146,147]
	–	g-func	–	–	–	–	[264]
Simulink	–	g-func	–	–	–	–	[158,175]
	–	EWS	–	–	–	–	[176]
DOE-2	–	g-func	–	–	–	–	[200,201]
VisualDOE[b]	–	–	–	–	PT	–	[144]
eQUEST[b]	–	g-func	–	–	–	–	[181,197,201]
ESP-r	ILS	–	–	–	–	–	[272]
TRNSYS–MATLAB	–	g-func	–	–	–	–	[211]
TRNSYS–FEFLOW	–	–	–	3D FEM	–	–	[130,208]
TRNSYS–COMSOL	–	–	–	–	–	2D FEM	[142,143]
EnergyPlus–Modelica	–	g-func	–	–	–	–	[206,207]
EnergyPlus–MATLAB	AN	–	–	–	–	–	[212]
EnergyPlus–Ansys Fluent	–	–	FVM	–	–	–	[139]
Modelica–TOUGH	–	2D FVM	–	–	–	–	[132,209]
	–	3D FVM	–	–	–	–	[186]
Modelica–FEFLOW	–	–	–	3D FEM	–	–	[187]
Modelica–OGS	–	3D FDM	–	–	–	–	[131,210]
COMFIE–MATLAB	–	g-func	–	–	–	–	[135]

[a] EnergyPlus based tool.
[b] DOE-2 based tool.

Data availability

No data was used for the research described in the article.

References

[1] International Energy Agency (IEA). https://www.iea.org [Accessed 30 January 2025].
[2] K.P. Tsagarakis, Shallow geothermal energy under the microscope: Social, economic, and institutional aspects, Renew. Energy 147 (2020) 2801–2808.
[3] A.C. Violante, F. Donato, G. Guidi, M. Proposito, Comparative life cycle assessment of the ground source heat pump vs air source heat pump, Renew. Energy 188 (2022) 1029–1037.
[4] K. Menberg, P. Bayer, K. Zosseder, S. Rumohr, P. Blum, Subsurface urban heat islands in German cities, Sci. Total Environ. 442 (2013) 123–133.
[5] M.D. Jackson, G. Regnier, I. Staffell, Aquifer thermal energy storage for low carbon heating and cooling in the United Kingdom: current status and future prospects, Appl. Energy 376 (2024) 124096.
[6] J.M. Chicco, D. Antonijevic, M. Bloemendal, F. Cecinato, G. Goetzl, M. Hajto, N. Hartog, G. Mandrone, D. Vacha, P.J. Vardon, Improving the Efficiency of District Heating and Cooling Using a Geothermal Technology: Underground Thermal Energy Storage (UTES), in: International Symposium: New Metropolitan Perspectives, Springer, 2022, pp. 1699-1710.
[7] R. Zeh, M. Schmid, B. Ohlsen, S. Venczel, V. Stockinger, 5th generation district heating and cooling networks as a heat source for geothermal heat pumps, Geothermal Heat Pump Systems, Springer (2023) 259–291.
[8] E. Zanetti, D. Blum, M. Wetter, Control development and sizing analysis for a 5th generation district heating and cooling, (2023).
[9] P. Blum, G. Campillo, T. Kölbel, Techno-economic and spatial analysis of vertical ground source heat pump systems in Germany, Energy 36 (5) (2011) 3002–3011.
[10] K. Allaerts, M. Coomans, R. Salenbien, Hybrid ground-source heat pump system with active air source regeneration, Energ. Conver. Manage. 90 (2015) 230–237.
[11] P. Bayer, G. Attard, P. Blum, K. Menberg, The geothermal potential of cities, Renew. Sustain. Energy Rev. 106 (2019) 17–30.
[12] G. Pallotta, E. Marrasso, C. Martone, N. Luciano, G. Squarzoni, C. Roselli, M. Sasso, Aquifer thermal energy storage for decarbonising heating and cooling energy supply in southern Europe: a dynamic environmental impact assessment, Appl. Energy 394 (2025) 126105.
[13] P.J. Ball, A review of geothermal technologies and their role in reducing greenhouse gas emissions in the USA, J. Energy Res. Technol. 143 (1) (2021) 010903.
[14] T. Sharmin, N.R. Khan, M.S. Akram, M.M. Ehsan, A state-of-the-art review on geothermal energy extraction, utilization, and improvement strategies: conventional, hybridized, and enhanced geothermal systems, Int. J. Thermofluids 18 (2023) 100323.
[15] E. Barbier, Geothermal energy technology and current status: an overview, Renew. Sustain. Energy Rev. 6 (1–2) (2002) 3–65.
[16] K. Menberg, S. Pfister, P. Blum, P. Bayer, A matter of meters: state of the art in the life cycle assessment of enhanced geothermal systems, Energ. Environ. Sci. 9 (9) (2016) 2720–2743.
[17] K. Menberg, F. Heberle, H. Uhrmann, C. Bott, S. Grünäugl, D. Brüggemann, P. Bayer, Environmental impact of cogeneration in binary geothermal plants, Renew. Energy 218 (2023) 119251.
[18] S. Wilke, K. Menberg, H. Steger, P. Blum, Advanced thermal response tests: a review, Renew. Sustain. Energy Rev. 119 (2020) 109575.
[19] P. Cui, W. Yang, W. Zhang, K. Zhu, J.D. Spitler, M. Yu, Advances in ground heat exchangers for space heating and cooling: Review and perspectives, Energy Built Environ. 5 (2) (2024) 255–269.
[20] T. Gao, X. Long, H. Xie, L. Sun, J. Wang, C. Li, M. Gao, E. Xia, A review of advances and applications of geothermal energy extraction using a gravity-assisted heat pipe, Geothermics 116 (2024) 102856.

[21] L. Kumar, M.S. Hossain, M.E.H. Assad, M.U. Manoo, Technological advancements and challenges of geothermal energy systems: a comprehensive review, Energies 15 (23) (2022) 9058.
[22] B.H. Al-Kbodi, T. Rajeh, Y. Li, J. Zhao, T. Zhao, M.E. Zayed, Heat extraction analyses and energy consumption characteristics of novel designs of geothermal borehole heat exchangers with elliptic and oval double U-tube structures, Appl. Therm. Eng. 235 (2023) 121418.
[23] Z. Cao, G. Zhang, Y. Wu, J. Yang, Y. Sui, X. Zhao, Energy storage potential analysis of phase change material (PCM) energy storage units based on tunnel lining ground heat exchangers, Appl. Therm. Eng. 235 (2023) 121403.
[24] S. Hähnlein, P. Bayer, G. Ferguson, P. Blum, Sustainability and policy for the thermal use of shallow geothermal energy, Energy Policy 59 (2013) 914–925.
[25] P. Dumas, Policy and regulatory aspects of geothermal energy: a European perspective, Geothermal Energy Soc. (2019) 19–37.
[26] T. Compernolle, K. Welkenhuysen, E. Petitclerc, D. Maes, K. Piessens, The impact of policy measures on profitability and risk in geothermal energy investments, Energy Econ. 84 (2019) 104524.
[27] H.M. Maghrabie, M.M. Abdeltwab, M.H.M. Tawfik, Ground-source heat pumps (GSHPs): Materials, models, applications, and sustainability, Energ. Buildings (2023) 113560.
[28] U. Lucia, M. Simonetti, G. Chiesa, G. Grisolia, Ground-source pump system for heating and cooling: review and thermodynamic approach, Renew. Sustain. Energy Rev. 70 (2017) 867–874.
[29] K. Menberg, A. Bidarmaghz, A. Gregory, R. Choudhary, M. Girolami, Multi-fidelity approach to Bayesian parameter estimation in subsurface heat and fluid transport models, Sci. Total Environ. 745 (2020) 140846.
[30] J. Gao, A. Li, X. Xu, W. Gang, T. Yan, Ground heat exchangers: applications, technology integration and potentials for zero energy buildings, Renew. Energy 128 (2018) 337–349.
[31] T. Yan, X. Xu, Utilization of ground heat exchangers: a review, Curr. Sustain./Renew. Energy Rep. 5 (2018) 189–198.
[32] N. Zhu, P. Hu, L. Xu, Z. Jiang, F. Lei, Recent research and applications of ground source heat pump integrated with thermal energy storage systems: a review, Appl. Therm. Eng. 71 (1) (2014) 142–151.
[33] J.S. Figueira, A.G. Gil, A. Vieira, A.K. Michopoulos, D.P. Boon, F. Loveridge, F. Cecinato, G. Götzl, J. Epting, K. Zosseder, Shallow geothermal energy systems for district heating and cooling networks: review and technological progression through case studies, Renew. Energy 236 (2024) 121436.
[34] A. Wallin, T. Thomasson, R. Abdurafikov, Urban low-to-medium deep borehole field regeneration with waste heat from energy efficient buildings: a techno-economic study in Nordic climate, Energ. Buildings 300 (2023) 113628.
[35] S.L. Do, J.S. Haberl, A review of ground coupled heat pump models used in whole-building computer simulation programs, (2010).
[36] A. Lyden, C. Brown, I. Kolo, G. Falcone, D. Friedrich, Seasonal thermal energy storage in smart energy systems: district-level applications and modelling approaches, Renew. Sustain. Energy Rev. 167 (2022) 112760.
[37] Z. Xia, G. Jia, Z. Ma, J. Wang, Y. Zhang, L. Jin, Analysis of economy, thermal efficiency and environmental impact of geothermal heating system based on life cycle assessments, Appl. Energy 303 (2021) 117671.
[38] S. Huang, D. Lin, J. Dong, J. Li, Effects of building load characteristics on heating performance of the medium-deep U-type borehole heat exchanger coupled heat pumps: a coupled dynamic simulation, Appl. Energy 377 (2025) 124405.
[39] ISO 13790: 2008-Energy performance of buildings-Calculation of energy use for space heating and cooling, Geneva, Switzerland, 2008.
[40] ANSI/ASHRAE, Standard 140-2023-Method of Test for Evaluating Building Performance Simulation Software, 2023.
[41] CEN, EN 15265: 2007: Energy Performance of Buildings–Calculation of Energy Needs for Space Heating and Cooling Using Dynamic Methods–General Criteria and Validation Procedures, CEN–European Committee for Standardization, Brussels, Belgium, 2007.
[42] J. Clarke, Energy simulation in building design, Routledge, 2007.
[43] J.F. Kreider, P.S. Curtiss, A. Rabl, Heating and cooling of buildings: design for efficiency, CRC Press, 2009.
[44] M. Magni, F. Ochs, S. de Vries, A. Maccarini, F. Sigg, Detailed cross comparison of building energy simulation tools results using a reference office building as a case study, Energ. Buildings 250 (2021) 111260.
[45] Y. Li, Z. O'Neill, L. Zhang, J. Chen, P. Im, J. DeGraw, Grey-box modeling and application for building energy simulations-a critical review, Renew. Sustain. Energy Rev. 146 (2021) 111174.
[46] L. Zhang, J. Wen, Y. Li, J. Chen, Y. Ye, Y. Fu, W. Livingood, A review of machine learning in building load prediction, Appl. Energy 285 (2021) 116452.
[47] E. Wang, A.S. Fung, C. Qi, W.H. Leong, Performance prediction of a hybrid solar ground-source heat pump system, Energ. Buildings 47 (2012) 600–611.
[48] L. Hu, Z.H. Rizvi, L. Tobber, F. Wuttke, Thermal performance of three horizontal ground heat exchanger systems: comparison of linear-loop, spiral-coil and slinky-coil arrangements, Front. Energy Res. 11 (2023) 1188506.
[49] R. Mirzanamadi, C.-E. Hagentoft, P. Johansson, Numerical investigation of harvesting solar energy and anti-icing road surfaces using a hydronic heating pavement and borehole thermal energy storage, Energies 11 (12) (2018) 3443.
[50] F. Simon, J. Ordoñez, T.A. Reddy, A. Girard, T. Muneer, Developing multiple regression models from the manufacturer's ground-source heat pump catalogue data, Renew. Energy 95 (2016) 413–421.
[51] S. Bordignon, J.D. Spitler, A. Zarrella, Simplified water-source heat pump models for predicting heat extraction and rejection, Renew. Energy 220 (2024) 119701.
[52] C. Underwood, Heat pump modelling, in: Advances in Ground-Source Heat Pump Systems, Elsevier, 2016, pp. 387-421.
[53] H. Pieper, I. Krupenski, W.B. Markussen, T. Ommen, A. Siirde, A. Volkova, Method of linear approximation of COP for heat pumps and chillers based on thermodynamic modelling and off-design operation, Energy 230 (2021) 120743.
[54] X. Xu, J. Liu, Y. Wang, J. Xu, J. Bao, Performance evaluation of ground source heat pump using linear and nonlinear regressions and artificial neural networks, Appl. Therm. Eng. 180 (2020) 115914.
[55] S. Lu, Q. Li, L. Bai, R. Wang, Performance predictions of ground source heat pump system based on random forest and back propagation neural network models, Energ. Conver. Manage. 197 (2019) 111864.
[56] S. Zhou, X. Chu, S. Cao, X. Liu, Y. Zhou, Prediction of the ground temperature with ANN, LS-SVM and fuzzy LS-SVM for GSHP application, Geothermics 84 (2020) 101757.
[57] H.U. Cho, Y. Nam, E.J. Choi, Y.J. Choi, H. Kim, S. Bae, J.W. Moon, Comparative analysis of the optimized ANN, SVM, and tree ensemble models using Bayesian optimization for predicting GSHP COP, J. Build. Eng. 44 (2021) 103411.
[58] M.T. Hughes, G. Kini, S. Garimella, Status, challenges, and potential for machine learning in understanding and applying heat transfer phenomena, J. Heat Transfer 143 (12) (2021) 120802.
[59] M.W. Ahmad, J. Reynolds, Y. Rezgui, Predictive modelling for solar thermal energy systems: a comparison of support vector regression, random forest, extra trees and regression trees, J. Clean. Prod. 203 (2018) 810–821.
[60] H. Yazdani, M. Baneshi, M. Yaghoubi, Techno-economic and environmental design of hybrid energy systems using multi-objective optimization and multi-criteria decision making methods, Energ. Conver. Manage. 282 (2023) 116873.
[61] Z. Wei, J. Calautit, Evaluation of model predictive control (MPC) of solar thermal heating system with thermal energy storage for buildings with highly variable occupancy levels, Building Simulation, Springer (2023) 1915–1931.
[62] H.T. Walnum, I. Sartori, P. Ward, S. Gros, Demonstration of a low-cost solution for implementing MPC in commercial buildings with legacy equipment, Appl. Energy 380 (2025) 125012.
[63] A. Toth, E. Bobok, Flow and heat transfer in geothermal systems: basic equations for describing and modeling geothermal phenomena and technologies, Elsevier, 2016.
[64] F. Stauffer, P. Bayer, P. Blum, N.M. Giraldo, W. Kinzelbach, Thermal use of shallow groundwater, CRC Press, 2013.
[65] J. Bear, Modeling phenomena of flow and transport in porous media, Springer, 2018.
[66] N. Cheng, C. Zhou, Y. Luo, J. Shen, Z. Tian, D. Sun, J. Fan, L. Zhang, J. Deng, M. A. Rosen, Thermal behavior and performance of shallow-deep-mixed borehole heat exchanger array for sustainable building cooling and heating, Energ. Buildings 291 (2023) 113108.
[67] J. Li, L. Bao, G. Niu, Z. Miao, X. Guo, W. Wang, Research on renewable energy coupling system based on medium-deep ground temperature attenuation, Appl. Energy 353 (2024) 122187.
[68] J. Liu, Y. Liu, C. Wang, C. Wang, Design and simulation analysis of solar-coupled ground source heat pump system, in, IOP Conference Series: Earth and Environmental Science, IOP Publishing (2020) 012039.
[69] Q. Liu, F. Weiland, P. Pärisch, N. Kracht, M. Huang, T. Ptak, Influence of site characteristics on the performance of shallow borehole heat exchanger arrays: a sensitivity analysis, Geothermics 114 (2023) 102785.
[70] O. Todorov, K. Alanne, M. Virtanen, R. Kosonen, A method and analysis of aquifer thermal energy storage (ATES) system for district heating and cooling: a case study in Finland, Sustain. Cities Soc. 53 (2020) 101977.
[71] A. Ferrantelli, J. Fadejev, J. Kurnitski, Energy pile field simulation in large buildings: Validation of surface boundary assumptions, Energies 12 (5) (2019) 770.
[72] Y. Elomari, G. Aspetakis, C. Mateu, A. Shobo, D. Boer, M. Marín-Genescà, Q. Wang, A hybrid data-driven co-simulation approach for enhanced integrations of renewables and thermal storage in building district energy systems, J. Build. Eng. (2025) 112405.
[73] E. Zanetti, D. Blum, M. Wetter, Control development and sizing analysis for a 5th generation district heating and cooling network using Modelica (2023).
[74] A. Jones, D. Finn, Co-simulation of a HVAC system-integrated phase change material thermal storage unit, J. Build. Perform. Simul. 10 (3) (2017) 313–325.
[75] Z. Cao, G. Zhang, J. Yang, X. Zhao, Long-term thermal performance investigation of phase change plates (PCPs) employing tunnel lining ground heat exchangers for cool storage, J. Clean. Prod. 447 (2024) 141494.
[76] X. Kang, D. Yan, X. Xie, J. An, Z. Liu, Co-simulation of dynamic underground heat transfer with building energy modeling based on equivalent slab method, Energ. Buildings 256 (2022) 111728.
[77] M. Busch, Zur effizienten Kopplung von Simulationsprogrammen, kassel University Press GmbH, 2012.
[78] Z. Hu, W. Tang, H. Xue, X. Zhang, A SIMPLE-based monolithic implicit method for strong-coupled fluid–structure interaction problems with free surfaces, Comput. Methods Appl. Mech. Eng. 299 (2016) 90–115.
[79] J. Kraft, S. Klimmek, T. Meyer, B. Schweizer, Implicit co-simulation and solver-coupling: efficient calculation of interface-Jacobian and coupling sensitivities/gradients, J. Comput. Nonlinear Dyn. 17 (4) (2022) 041004.
[80] M. Venzke, Y. Shudrenko, A. Youssfi, T. Steffen, V. Turau, C. Becker, Co-simulation of a cellular energy system, Energies 16 (17) (2023) 6150.
[81] D.L. Fernandes, A.L.M. Leopoldino, J. de Santiago, C. Verginis, A.A. Ferreira, J. G. de Oliveira, Distributed control on a multi-agent environment co-simulation for DC bus voltage control, Electr. Pow. Syst. Res. 232 (2024) 110408.
[82] J. Kampars, D. Tropins, R. Matisons, A review of application layer communication protocols for the iot edge cloud continuum, in: In: 2021 62nd International

Scientific Conference on Information Technology and Management Science of Riga Technical University (ITMS), 2021, pp. 1–6.
[83] Functional Mock-up Interface (FMI). https://fmi-standard.org [Accessed 3 June 2025].
[84] P. Riederer, W. Keilholz, V. Ducreux, Coupling of TRNSYS with Simulink–a method to automatically export and use TRNSYS models within Simulink and vice versa, (2009).
[85] L.I. Hatledal, A. Styve, G. Hovland, H. Zhang, A language and platform independent co-simulation framework based on the functional mock-up interface, IEEE Access 7 (2019) 109328–109339.
[86] S.A. Klein, TRNSYS-A transient system simulation program, University of Wisconsin-Madison, Engineering Experiment Station Report (1988) 38.
[87] Z. Li, Y. Xie, H. Zhu, Influence of Battery Life Degradation on Pv Battery Capacity Configuration in Urban Industrial Park in Shanghai, Available at SSRN 4791801.
[88] D.B. Crawley, L.K. Lawrie, F.C. Winkelmann, W.F. Buhl, Y.J. Huang, C. O. Pedersen, R.K. Strand, R.J. Liesen, D.E. Fisher, M.J. Witte, EnergyPlus: creating a new-generation building energy simulation program, Energ. Buildings 33 (4) (2001) 319–331.
[89] P. Usta, B. Zengin, Energy assessment of different building materials in the education building, Energy Rep. 7 (2021) 603–608.
[90] S.K. Alghoul, A comparative study of energy consumption for residential hvac systems using EnergyPlus, American Journal of Mechanical and Industrial Engineering 2 (2) (2017) 98–103.
[91] M. Wetter, K. Benne, H. Tummescheit, C. Winther, Spawn: coupling Modelica buildings Library and EnergyPlus to enable new energy system and control applications, J. Build. Perform. Simul. 17 (2) (2024) 274–292.
[92] IDA Indoor Climate and Energy (IDA ICE). https://www.equa.se [Accessed 9 January 2025].
[93] T. Arghand, S. Javed, J.-O. Dalenbäck, Combining direct ground cooling with ground-source heat pumps and district heating: Energy and economic analysis, Energy 270 (2023) 126944.
[94] C. Wang, Q. Wang, B. Nourozi, H. Pieskä, A. Ploskić, Evaluating the cooling potential of a geothermal-assisted ventilation system for multi-family dwellings in the scandinavian climate, Build. Environ. 204 (2021) 108114.
[95] M. Rabani, H.B. Madessa, J. Torgersen, N. Nord, Parametric analysis of ground source heat pump system for heating of office buildings in Nordic climate, in: International Conference Organised by IBPSA-Nordic, 13th–14th October 2020, OsloMet. BuildSIM-Nordic 2020. Selected papers, 2020.
[96] P. Fritzson, V. Engelson, in: Modelica—A Unified Object-Oriented Language for System Modeling and Simulation, in: ECOOP'98—Object-Oriented Programming, Springer, 1998, pp. 67–90.
[97] J. Wang, X. Niu, R.X. Gao, Z. Huang, R. Xue, Digital twin-driven virtual commissioning of machine tool, Rob. Comput. Integr. Manuf. 81 (2023) 102499.
[98] CARNOT Toolbox Ver. 8.02. For MATLAB/Simulink R2021b. Solar-Institut Jülich. https://www.fh-aachen.de/forschung/institute/sij/carnot [Accessed 9 January 2025].
[99] D. Siegele, E. Leonardi, F. Ochs, A new MATLAB Simulink Toolbox for Dynamic Building Simulation with BIM and Hardware in the Loop compatibility, in: Building Simulation 2019, IBPSA, 2019, pp. 2651-2658.
[100] M. De Wit, Hambase: heat, air and moisture model for building and systems evaluation, (2006).
[101] J.P. Campana, G.L. Morini, Bestest and EN ISO 52016 benchmarking of almabuild, a new open-source simulink tool for dynamic energy modelling of buildings, Energies 12 (15) (2019) 2938.
[102] B. Welsch, W. Rühaak, D.O. Schulte, J. Formhals, K. Bär, I. Sass, Co-simulation of geothermal applications and HVAC systems, Energy Procedia 125 (2017) 345–352.
[103] C. Natale, C. Naldi, M. Dongellini, G. Morini, Long term performance analysis of a Dual-Source Heat Pump system by means of the Matlab/Simulink tool ALMABuild, in: In: 14th IEA Heat Pump Conference 2023 (HPC2023) Conference Proceedings, 2023, pp. 1–12.
[104] B. Birdsall, W. Buh, K. Ellington, A. Erem, F. Winkelmann, DOE-2. BASIC, Version 2.1 E, (1994).
[105] D. Zhu, T. Hong, D. Yan, C. Wang, A detailed loads comparison of three building energy modeling programs: EnergyPlus, DeST and DOE-2.1 E, in, Building Simulation, Springer (2013) 323–335.
[106] X. Zhou, T. Hong, D. Yan, Comparison of HVAC system modeling in EnergyPlus, DeST and DOE-2.1 E, in, Building Simulation, Springer (2014) 21–33.
[107] C.I. Seyrek, B. Widera, A. Woźniczka, Sustainability-related parameters and decision support tools for kinetic green façades, Sustainability 13 (18) (2021) 10313.
[108] K. Lee, I. Kim, S. Choo, Model study of design components for energy-performance-based architectural design using BIM LOD 100, Journal of Green Building 10 (2) (2015) 179–197.
[109] P. Strachan, G. Kokogiannakis, I. Macdonald, History and development of validation with the ESP-r simulation program, Build. Environ. 43 (4) (2008) 601–609.
[110] K.A. Barber, M. Krarti, A review of optimization based tools for design and control of building energy systems, Renew. Sustain. Energy Rev. 160 (2022) 112359.
[111] J. Purdy, A. Morrison, Ground-source heat pump simulation within a whole-building analysis, in, Eighth International IBPSA Conference (2003) 11–14.
[112] D. Thevenard, K. Haddad, J. Purdy, Development of a new solar collector model in ESP-r, in: Canadian Solar Buildings Conference, Montreal, Canada, 2004.
[113] F. Jawara, A. Seeam, V. Ramsurrun, Performance Comparison of ESP-r in Containers vs Virtual Machines for Digital Twins, in: 2024 International Conference on Artificial Intelligence, Big Data, Computing and Data Communication Systems (icABCD), IEEE, 2024, pp. 1-6.
[114] B. Peuportier, I.B. Sommereux, Simulation tool with its expert interface for the thermal design of multizone buildings, International Journal of Solar Energy 8 (2) (1990) 109–120.
[115] L. Pei, P. Schalbart, B. Peuportier, Quantitative evaluation of the effects of heat island on building energy simulation: a case study in Wuhan, China, Energies 16 (7) (2023) 3032.
[116] M. Frossard, P. Schalbart, B. Peuportier, Dynamic and consequential LCA aspects in multi-objective optimisation for NZEB design, in, IOP Conference Series: Earth and Environmental Science, IOP Publishing (2020) 032031.
[117] F. Witte, I. Tuschy, Tespy: thermal engineering systems in python, Journal of Open Source Software 5 (49) (2020) 2178.
[118] D. Maldonado, P. Schönfeldt, H. Torio, F. Witte, M. Füting, Validation of a calibrated steady-state heat network model using measured data, Appl. Therm. Eng. 248 (2024) 123267.
[119] L. Vorspel, J. Bücker, District-heating-grid simulation in python: Digripy, Computation 9 (6) (2021) 72.
[120] J. Hecht-Méndez, N. Molina-Giraldo, P. Blum, P. Bayer, Evaluating MT3DMS for heat transport simulation of closed geothermal systems, Groundwater 48 (5) (2010) 741–756.
[121] C.D. Langevin, D.T. Thorne Jr, A.M. Dausman, M.C. Sukop, W. Guo, SEAWAT version 4: a computer program for simulation of multi-species solute and heat transport, in, Geological Survey (US) (2008).
[122] J.E. Matsson, An introduction to ANSYS fluent 2022, Sdc Publications (2022).
[123] I. Guide, Comsol Multiphysics, 5.6, COMSOL AB (1998) 204–208.
[124] H.-J.-G. Diersch, Feflow: finite element modeling of flow, mass and heat transport in porous and fractured media, Springer Science & Business Media, 2013.
[125] K.-A. Lie, An introduction to reservoir simulation using MATLAB/GNU Octave: User guide for the MATLAB Reservoir simulation Toolbox (MRST), Cambridge University Press, 2019.
[126] L. Bilke, C. Lehmann, D. Naumov, T. Fischer, W. Wang, J. Buchwald, K. Rink, N. Grunwald, F. Zill, F.K. Kiszkurno, OpenGeoSys, Zenodo, (2022).
[127] A.W. Harbaugh, MODFLOW-2005, the US Geological Survey modular ground-water model: the ground-water flow process, US Department of the Interior, US Geological Survey Reston, VA, USA, 2005.
[128] K. Pruess, TOUGH user's guide, (1987).
[129] Building Controls Virtual Test Bed (BCVTB). https://simulationresearch.lbl.gov/bcvtb [Accessed 3 June 2025].
[130] H.-J. Diersch, D. Bauer, W. Heidemann, W. Rühaak, P. Schätzl, Finite element modeling of borehole heat exchanger systems: Part 2, Numerical Simulation, Computers & Geosciences 37 (8) (2011) 1136–1147.
[131] J. Randow, P. Satke, M. Jaeschke, A. Bucher, O. Kolditz, H. Shao, S. Schoenfelder, A software interface for coupled underground and facility simulations between OpenGeoSys and Modelica, J. Build. Perform. Simul. (2025) 1–19.
[132] J. Hu, C. Doughty, P. Dobson, P. Nico, M. Wetter, Coupling subsurface and above-surface models for design of borefields and geothermal district heating and cooling systems. In: Proceedings, 45th Workshop on Geothermal Reservoir Engineering, 2020.
[133] W. Cai, F. Wang, C. Chen, S. Chen, J. Liu, Z. Ren, H. Shao, Long-term performance evaluation for deep borehole heat exchanger array under different soil thermal properties and system layouts, Energy 241 (2022) 122937.
[134] J.D. Hughes, M.J. Russcher, C.D. Langevin, E.D. Morway, R.R. McDonald, The MODFLOW Application programming Interface for simulation control and software interoperability, Environ. Model. Software 148 (2022) 105257.
[135] L. Pei, P. Schalbart, B. Peuportier, Modelling of a Large Vertical Ground Heat Exchanger Integrated with a Heat Pump for Building Energy simulation in China, in, IOP Conference Series: Earth and Environmental Science, IOP Publishing (2020) 022050.
[136] A. Dahash, F. Ochs, A. Tosatto, Co-simulation of dynamic energy system simulation and COMSOL multiphysics®, in, COMSOL Conference (2019).
[137] M.Y. Ferroukhi, R. Djedjig, K. Limam, R. Belarbi, Hygrothermal behavior modeling of the hygroscopic envelopes of buildings: a dynamic co-simulation approach, in, Building Simulation, Springer (2016) 501–512.
[138] B.C. Kwag, M. Krarti, Evaluation of thermo-active foundations for heating and cooling residential buildings, J. Sol. Energy Eng. 138 (6) (2016) 061010.
[139] P. Adebayo, C. Beragama Jathunge, R. Shor, A. Mohamad, A. Mwesigye, A Comparative Study of the Long-Term Performance of Vertical U-Tube Borehole Heat Exchanger and Foundation Piles in a Cold Climate, in: ASME International Mechanical Engineering Congress and Exposition, American Society of Mechanical Engineers, 2023, pp. V007T008A011.
[140] S. Kranz, S. Frick, Efficient cooling energy supply with aquifer thermal energy storages, Appl. Energy 109 (2013) 321–327.
[141] G. Drenkelfort, S. Kieseler, A. Pasemann, F. Behrendt, Aquifer thermal energy storages as a cooling option for German data centers, Energ. Effi. 8 (2015) 385–402.
[142] B. Bozkaya, R. Li, W. Zeiler, A dynamic building and aquifer co-simulation method for thermal imbalance investigation, Appl. Therm. Eng. 144 (2018) 681–694.
[143] B. Bozkaya, W. Zeiler, The energy efficient use of an air handling unit for balancing an aquifer thermal energy storage system, Renew. Energy 146 (2020) 1932–1942.
[144] S. Ferrari, G. Masera, D. Dell'Oro, Improving comfort and energy efficiency in a nursery school design process, in. Proceedings of PLEA 2006—23rd International Conference on Passive and Low Energy Architecture, 2006.

[145] R. Miao, G. Olson, D. Selby, X. Hu, Use of solar thermal collectors and a horizontal underground loop in a multi-source heat pump system for thermal energy storage, ASHRAE Trans. 126 (2020) 556–564.
[146] D. D'Agostino, F. Minichiello, F. Petito, C. Renno, A. Valentino, Retrofit strategies to obtain a NZEB using low enthalpy geothermal energy systems, Energy 239 (2022) 122307.
[147] R. Stasi, F. Ruggiero, U. Berardi, The efficiency of hybrid ventilation on cooling energy savings in NZEBs, J. Build. Eng. 53 (2022) 104401.
[148] N. Nord, L.H. Qvistgaard, G. Cao, Identifying key design parameters of the integrated energy system for a residential Zero Emission Building in Norway, Renew. Energy 87 (2016) 1076–1087.
[149] S. Bordignon, G. Emmi, A. Zarrella, M. De Carli, Energy analysis of different configurations for a reversible ground source heat pump using a new flexible TRNSYS Type, Appl. Therm. Eng. 197 (2021) 117413.
[150] E. Marrasso, C. Roselli, M. Sasso, F. Tariello, Global and local environmental and energy advantages of a geothermal heat pump interacting with a low temperature thermal micro grid, Energ. Conver. Manage. 172 (2018) 540–553.
[151] M. Canelli, E. Entchev, M. Sasso, L. Yang, M. Ghorab, Dynamic simulations of hybrid energy systems in load sharing application, Appl. Therm. Eng. 78 (2015) 315–325.
[152] A. Nešović, N. Jurišević, R. Kowalik, I. Terzić, Potential of contemporary earth-sheltered buildings to achieve Plus Energy status in various European climates during the heating season, Building Simulation, Springer (2024) 41–52.
[153] P. Valdiserri, M. Lucchi, M. Lorenzini, Energy and exergy analysis of a HVAC system having a ground source heat pump as generation system, Building Simulation Applications BSA... (2020, 2020,) 165–172.
[154] B. Buonomo, V. Ciccarelli, O. Manca, S. Nardini, R. Plomitallo, Effect of nanofluid on a Low-enthalpy geothermal plant, J. Phys.: Conf. Ser., IOP Publishing (2022) 012018.
[155] A. Zarrella, R. Zecchin, F. De Rossi, G. Emmi, M. De Carli, L. Carnieletto, Analysis of a double source heat pump system in a historical building, in, Building Simulation Conference Proceedings, International Building Performance Simulation Association (2020) 1778–1785.
[156] J.M. Corberán, A. Cazorla-Marín, J. Marchante-Avellaneda, C. Montagud, Dual source heat pump, a high efficiency and cost-effective alternative for heating, cooling and DHW production, International Journal of Low-Carbon Technologies 13 (2) (2018) 161–176.
[157] I. Grossi, M. Dongellini, A. Piazzi, G.L. Morini, Dynamic modelling and energy performance analysis of an innovative dual-source heat pump system, Appl. Therm. Eng. 142 (2018) 745–759.
[158] C. Natale, C. Naldi, M. Dongellini, G.L. Morini, Dynamic modelling of a dual-source heat pump system through a Simulink tool, J. Phys.: Conf. Ser., IOP Publishing (2022) 012090.
[159] T. Arghand, S. Javed, J.-O. Dalenbäck, Combining direct ground cooling with ground-source heat pumps and district heating: Borehole sizing and land area requirements, Geothermics 106 (2022) 102565.
[160] P. McKenna, W.J. Turner, D. Finn, Geocooling with integrated PCM thermal energy storage in a commercial building, Energy 144 (2018) 865–876.
[161] F. Reda, N. Arcuri, P. Loiacono, D. Mazzeo, Energy assessment of solar technologies coupled with a ground source heat pump system for residential energy supply in southern European climates, Energy 91 (2015) 294–305.
[162] V. Battaglia, L. Vanoli, C. Verde, P. Nithiarasu, J.R. Searle, Dynamic modelling of geothermal heat pump system coupled with positive-energy building, Energy 284 (2023) 128557.
[163] K. Januševičius, G. Streckienė, Solar assisted ground source heat pump performance in nearly zero energy building in Baltic countries, Environ. Clim. Technol. 11 (2013) (2013) 48–56.
[164] Y.J. Nam, X.Y. Gao, S.H. Yoon, K.H. Lee, Study on the performance of a ground source heat pump system assisted by solar thermal storage, Energies 8 (12) (2015) 13378–13394.
[165] F. Reda, Long term performance of different SAGSHP solutions for residential energy supply in Finland, Appl. Energy 144 (2015) 31–50.
[166] A. Berkane, M. Aksas, Z. Aouachria, Performance study of a hybrid solar-assisted ground-source heat pump system used for building heating and hot water demands, Jordan J. Mech. Indus. Eng. 17 (4) (2023).
[167] M. Ferrara, E. Fabrizio, Optimized design and integration of energy storage in Solar-Assisted Ground-Source Heat Pump systems, Building Simulation, Springer (2023) 1933–1948.
[168] Y. Chen, Z. Chen, Z. Chen, X. Yuan, Dynamic modeling of solar-assisted ground source heat pump using Modelica, Appl. Therm. Eng. 196 (2021) 117324.
[169] N. Wang, K. Liu, J. Hu, X. Wang, Simulation of operation performance of a solar assisted ground heat pump system with phase change thermal storage for heating in a rural building in Xi'an, IOP Conference Series: Earth and Environmental Science, IOP Publishing (2019) 012062.
[170] L. Xu, F. Guo, P.-J. Hoes, X. Yang, J.L. Hensen, Investigating energy performance of large-scale seasonal storage in the district heating system of chifeng city: Measurements and model-based analysis of operation strategies, Energ. Buildings 247 (2021) 111113.
[171] W. Yaïci, A. Annuk, E. Entchev, M. Longo, J. Kalder, Organic Rankine cycle-ground source heat pump with seasonal energy storage based micro-cogeneration system in cold climates: the case for Canada, Energies 14 (18) (2021) 5705.
[172] F. Wang, T. You, Synergetic performance improvement of a novel building integrated photovoltaic/thermal-energy pile system for co-utilization of solar and shallow-geothermal energy, Energ. Conver. Manage. 288 (2023) 117116.
[173] J. Fadejev, R. Simson, J. Kurnitski, J. Kesti, Heat recovery from exhaust air as a thermal storage energy source for geothermal energy piles, Energy Procedia 96 (2016) 478–488.
[174] Q. Si, M. Okumiya, X. Zhang, Performance evaluation and optimization of a novel solar-ground source heat pump system, Energ. Buildings 70 (2014) 237–245.
[175] J.L. Gaspredes, G.Y. Masada, T.J. Moon, A Simulink®-based building load-ground source heat pump model used to assess short-and long-term heat pump and ground loop performance, J. Therm. Sci. Eng. Appl. 6 (2) (2014) 021013.
[176] R. Dott, C. Wemhöner, T. Afjei, Hydraulics, performance and comfort of ground coupled heating-cooling systems, (2007).
[177] H. Kauko, M.J. Alonso, O. Stavset, I.C. Claussen, Case study on residential building renovation and its impact on the energy use and thermal comfort, Energy Procedia 58 (2014) 160–165.
[178] W. Wu, H.M. Skye, P.A. Domanski, Selecting HVAC systems to achieve comfortable and cost-effective residential net-zero energy buildings, Appl. Energy 212 (2018) 577–591.
[179] L. Xing, C. Ren, H. Luo, Y. Guan, D. Li, L. Yan, Y. Miao, P. Hu, Feasibility of Hybrid Ground Source Heat Pump Systems Utilizing Capillary Radiation Roof Terminal in the Yangtze River Basin of China, in: Proceedings of the 11th International Symposium on Heating, Ventilation and Air Conditioning (ISHVAC 2019) Volume II: Heating, Ventilation, Air Conditioning and Refrigeration System 11, Springer, 2020, pp. 621-629.
[180] L. Xing, P. Hu, Simulation of hybrid GSHP systems utilizing radiant ceiling terminal and system evaluation with analytic hierarchy process method, Indoor Built Environ. 29 (9) (2020) 1202–1213.
[181] J. Chen, J. Peng, G. Zhang, J. Zhou, The utilization of GSHP in the Vangtze river area, (2007).
[182] M. Kummert, M. Bernier, Sub-hourly simulation of residential ground coupled heat pump systems, Build. Serv. Eng. Res. Technol. 29 (1) (2008) 27–44.
[183] C. Montagud, J.M. Corberán, F. Ruiz-Calvo, Experimental and modeling analysis of a ground source heat pump system, Appl. Energy 109 (2013) 328–336.
[184] G. Hou, H. Taherian, Performance analysis of a hybrid ground source heat pump system integrated with liquid dry cooler, Appl. Therm. Eng. 159 (2019) 113830.
[185] A. Zarrella, R. Zecchin, P. Pasquier, D. Guzzon, M. De Carli, G. Emmi, M. Quaggia, A comparison of numerical simulation methods analyzing the performance of a ground-coupled heat pump system, Sci. Technol. Built Environ. 24 (5) (2018) 502–512.
[186] J. Hu, C. Doughty, P. Dobson, P. Nico, M. Wetter, Coupling subsurface and above-surface models for optimizing the design of borefields and district heating and cooling systems in the presence of moving groundwater, (2022).
[187] J. Formhals, B. Welsch, H. Hemmatabady, D.O. Schulte, L. Seib, I. Sass, Co-simulation of district heating systems and borehole heat exchanger arrays using 3D finite element method subsurface models, J. Build. Perform. Simul. 15 (3) (2022) 362–378.
[188] M. Li, K. Zhu, Y. Lu, Q. Zhao, K. Yin, Technical and economic analysis of multi-energy complementary systems for net-zero energy consumption combining wind, solar, hydrogen, geothermal, and storage energy, Energ. Conver. Manage. 295 (2023) 117572.
[189] G. Qiu, K. Li, W. Cai, S. Yu, Optimization of an integrated system including a photovoltaic/thermal system and a ground source heat pump system for building energy supply in cold areas, Appl. Energy 349 (2023) 121698.
[190] I. Cupeiro Figueroa, M. Cimmino, L. Helsen, A methodology for long-term model predictive control of hybrid geothermal systems: the shadow-cost formulation, Energies 13 (23) (2020) 6203.
[191] Y. Lin, H. Wang, P. Hu, W. Yang, Q. Hu, N. Zhu, F. Lei, A study on the optimal air, load and source side temperature combination for a variable air and water volume ground source heat pump system, Appl. Therm. Eng. 178 (2020) 115595.
[192] I.C. Figueroa, D. Picard, L. Helsen, Short-term modeling of hybrid geothermal systems for model predictive control, Energ. Buildings 215 (2020) 109884.
[193] L. Hermans, W. Boydens, L. Helsen, Sizing of optimally controlled district heating systems: effect of district size and occupancy heterogeneity, in: Building Simulation 2023, IBPSA, 2023, pp. 2800-2807.
[194] G. Hou, H. Taherian, L. Li, J. Fuse, L. Moradi, System performance analysis of a hybrid ground source heat pump with optimal control strategies based on numerical simulations, Geothermics 86 (2020) 101849.
[195] F. Ruiz-Calvo, C. Montagud, A. Cazorla-Marín, J.M. Corberán, Development and experimental validation of a TRNSYS dynamic tool for design and energy optimization of ground source heat pump systems, Energies 10 (10) (2017) 1510.
[196] F. Calise, F.L. Cappiello, M.D. d'Accadia, M. Vicidomini, Energy and economic analysis of a small hybrid solar-geothermal trigeneration system: a dynamic approach, Energy 208 (2020) 118295.
[197] P. Shen, J.R. Lukes, Impact of global warming on performance of ground source heat pumps in US climate zones, Energ. Conver. Manage. 101 (2015) 632–643.
[198] A. Zajacs, K. Lebedeva, R. Bogdanovičs, Evaluation of Heat Pump operation in a Single-Family House, Latv. J. Phys. Tech. Sci. 60 (3) (2023) 85–98.
[199] K. Ooi, P.X. Zou, M.O. Abdullah, A simulation study of passively heated residential buildings, Procedia Eng. 121 (2015) 749–756.
[200] W. Ryan, M. Czachorski, An economic analysis of conventional and heat pump heating and cooling systems in the DOE prototypical elementary school building in various climatic zones, ASHRAE Trans. 121 (2) (2015).
[201] S.L. Do, J. Haberl, Development of a ground-coupled heat pump system simulation model using g-function approximation for a residential code-compliant tool, in, Building Simulation, Springer (2018) 51–66.
[202] P. Eskilson, Thermal analysis of heat extraction boreholes, (1987).

[203] J. Claesson, S. Javed, An Analytical Method to Calculate Borehole Fluid Temperatures for Time-scales from Minutes to decades, ASHRAE Trans. 117 (2) (2011).
[204] M. Cimmino, Semi-Analytical Method for g-Function Calculation of bore fields with series-and parallel-connected boreholes, Sci. Technol. Built Environ. 25 (8) (2019) 1007–1022.
[205] J. Wei, L. Wang, L. Jia, W. Cai, A new method for calculation of short time-step g-functions of vertical ground heat exchangers, Appl. Therm. Eng. 99 (2016) 776–783.
[206] A. Gautier, M. Wetter, M. Sulzer, Resilient cooling through geothermal district energy system, Appl. Energy 325 (2022) 119880.
[207] G. Cucca, A. Ianakiev, Assessment and optimisation of energy consumption in building communities using an innovative co-simulation tool, J. Build. Eng. 32 (2020) 101681.
[208] H. Langevin, N. Giordano, J. Raymond, L. Gosselin, M. Bourbonnais, Geothermal heat pumps to reduce diesel consumption in an off-grid subarctic community: Comparison of solar assisted systems with optional underground energy storage, Geothermics 116 (2024) 102846.
[209] C. Doughtry, J. Hu, P. Dobson, P. Nico, M. Wetter, Coupling subsurface and above-surface models for optimizing the design of borefields and district heating and cooling systems in the presence of varying water-table depth. In: Proceedings, 46th Workshop on Geothermal Reservoir Engineering, in, Lawrence Berkeley National Lab.(LBNL), Berkeley, CA (United States), 2022.
[210] P. Satke, J. Randow, M. Jäschke, S. Schönfelder, Analyse von Haustechnikkomponenten, in: EASyQuart-Energieeffiziente Auslegung und Planung dezentraler Versorgungsnetze von Stadtquartieren: Heizen und Kühlen unter Nutzung oberflächennaher geologischer Ressourcen, Springer, 2023, pp. 149-200.
[211] O. Alaie, R. Maddahian, G. Heidarinejad, Investigation of thermal interaction between shallow boreholes in a GSHE using the FLS-STRCM model, Renew. Energy 175 (2021) 1137–1150.
[212] A. Kharbouch, S. Berrabah, M. Bakhouya, J. Gaber, D. El Ouadghiri, S. Idrissi Kaitouni, Experimental and co-simulation performance evaluation of an earth-to-air heat exchanger system integrated into a smart building, Energies 15 (15) (2022) 5407.
[213] A. Guideline, Measurement of energy, demand, and water savings, ASHRAE Guidel 4 (2014) 1–150.
[214] J. Cowan, International performance measurement and verification protocol: Concepts and Options for Determining Energy and Water Savings-Vol. I, International Performance Measurement & Verification Protocol, 1 (2002).
[215] K. Aljundi, A. Figueiredo, A. Vieira, J. Lapa, R. Cardoso, Geothermal energy system application: from basic standard performance to sustainability reflection, Renew. Energy 220 (2024) 119612.
[216] M.J. Kim, B.M. Seo, J.M. Lee, J.M. Choi, K.H. Lee, Operational behavior characteristics and energy saving potential of vertical closed loop ground source heat pump system combined with storage tank in an office building, Energ. Buildings 179 (2018) 239–252.
[217] S. Cho, S. Mirianhosseinabadi, Simulation modeling of ground source heat pump systems for the performance analysis of residential buildings, (2013).
[218] N.N. Thanh, P. Thunyawatcharakul, N.H. Ngu, S. Chotpantarat, Global review of groundwater potential models in the last decade: parameters, model techniques, and validation, J. Hydrol. 614 (2022) 128501.
[219] Deutscher Verein des Gas- und Wasserfaches (DVGW), Technische Regel – Arbeitsblatt DVGW W 107 (A). Aufbau und Anwendung numerischer Grundwassermodelle in Wassergewinnungsgebieten, 2016.
[220] X. Yang, W. Cai, Y. Li, M. Wang, Y. Kong, F. Wang, C. Chen, Numerical investigation on the influence of groundwater flow on long-term heat extraction performance of deep borehole heat exchanger array, Geotherm. Energy 12 (1) (2024) 45.
[221] N. Molina-Giraldo, P. Blum, K. Zhu, P. Bayer, Z. Fang, A moving finite line source model to simulate borehole heat exchangers with groundwater advection, Int. J. Therm. Sci. 50 (12) (2011) 2506–2513.
[222] J.A. Rivera, P. Blum, P. Bayer, A finite line source model with Cauchy-type top boundary conditions for simulating near surface effects on borehole heat exchangers, Energy 98 (2016) 50–63.
[223] M. Sulzer, M. Wetter, R. Mutschler, A. Sangiovanni-Vincentelli, Platform-based design for energy systems, Appl. Energy 352 (2023) 121955.
[224] TESS Component Library Package. https://www.trnsys.com/tess-libraries/GeneralDescriptions_TESSLibs18.pdf [Accessed 19 January 2025].
[225] Transsolar Software Engineering. https://trnsys.de [Accessed 19 January 2025].
[226] EnergyPlus™ Version 24.2.0 Documentation. Engineering Reference. U.S. Department of Energy. https://energyplus.net [Accessed 19 January 2025].
[227] DOE-2. Building Energy Use and Cost Analysis Tool. https://doe2.com [Accessed 9 January 2025].
[228] J.E. Bose, M.D. Smith, Performance of new ground heat exchanger configurations for heat pumps, Solar Eng. 1 (1992).
[229] G. Hellstrom, Ground heat storage: Thermal analyses of duct storage systems. I. Theory, (1992).
[230] S. Chapuis, Stockage thermique saisonnier dans un champ de puits géothermiques verticaux en boucle fermée, École Polytechnique De Montréal (2009).
[231] S. Chapuis, M. Bernier, Seasonal storage of solar energy in borehole heat exchangers, in: Building Simulation 2009, IBPSA, 2009, pp. 599-606.
[232] D. Pahud, A. Fromentin, J. Hadorn, The superposition borehole model for TRNSYS (TRNSBM), User Manuel, Internal Report, LASEN-EPFL, Lausanne, 1996.
[233] M. Wetter, A. Huber, TRNSYS Type 451: Vertical borehole heat exchanger EWS model, Version 3.1-model description and implementing into TRNSYS, Transsolar GmbH, Stuttgart, Germany, (1997).
[234] A. Murugappan, Implementing ground source heat pump and ground loop heat exchanger models in the EnergyPlus simulation environment, Citeseer (2002).
[235] D. Bauer, W. Heidemann, H. Müller-Steinhagen, H.J. Diersch, Thermal resistance and capacity models for borehole heat exchangers, Int. J. Energy Res. 35 (4) (2011) 312–320.
[236] Modelica Documentation. https://build.openmodelica.org/Documentation/Buildings.Fluid.Geothermal.Boreholes.UTube.html [Accessed 9 January 2025].
[237] S. Javed, Thermal modelling and evaluation of borehole heat transfer, Chalmers Tekniska Hogskola (Sweden) (2012).
[238] M. Cimmino, Fast calculation of the g-functions of geothermal borehole fields using similarities in the evaluation of the finite line source solution, J. Build. Perform. Simul. 11 (6) (2018) 655–668.
[239] M. Li, P. Li, V. Chan, A.C. Lai, Full-scale temperature response function (G-function) for heat transfer by borehole ground heat exchangers (GHEs) from sub-hour to decades, Appl. Energy 136 (2014) 197–205.
[240] Modelica Documentation. https://build.openmodelica.org/Documentation/IDEAS.Fluid.Geothermal.Borefields.BaseClasses.HeatTransfer.ThermalResponseFactors.gFunction.html [Accessed 19 January 2025].
[241] J. Formhals, H. Hemmatabady, B. Welsch, D.O. Schulte, I. Sass, A modelica toolbox for the simulation of borehole thermal energy storage systems, Energies 13 (9) (2020) 2327.
[242] J. Fadejev, J. Kurnitski, Geothermal energy piles and boreholes design with heat pump in a whole building simulation software, Energ. Buildings 106 (2015) 23–34.
[243] Boreholes model in IDA-ICE. https://www.equa.se/en/ida-ice/extensions/borehole [Accessed 19 January 2025].
[244] X. Liu, G. Hellstrom, Enhancements of an integrated simulation tool for ground-source heat pump system design and energy analysis, Proceedings of Ecostock (2006).
[245] D. Pahud, A. Fromentin, J. Hadorn, The duct ground heat storage model (DST) for TRNSYS used for the simulation of heat exchanger piles, DGC-LASEN, Lausanne, (1996).
[246] T. Schmidt, Aquifer Thermal Energy Storage–TRNAST Two Well Model for TRNSYS, Stuttgart: Solites—Steinbeis Research Institute for Solar and Sustainable Thermal Energy Systems, (2005).
[247] A. Ahmed, K. Ip, A. Miller, K. Gidado, Thermal performance of earth-air heat exchanger for reducing cooling energy demand of office buildings in the United Kingdom, (2009).
[248] T. Arghand, S. Javed, A. Trüschel, J.-O. Dalenbäck, A comparative study on borehole heat exchanger size for direct ground coupled cooling systems using active chilled beams and TABS, Energ. Buildings 240 (2021) 110874.
[249] T. Arghand, S. Javed, A. Trüschel, J.-O. Dalenbäck, Cooling of office buildings in cold climates using direct ground-coupled active chilled beams, Renew. Energy 164 (2021) 122–132.
[250] T. Arghand, S. Javed, A. Trüschel, J.-O. Dalenbäck, Influence of system operation on the design and performance of a direct ground-coupled cooling system, Energ. Buildings 234 (2021) 110709.
[251] O. Zogou, A. Stamatelos, Optimization of thermal performance of a building with ground source heat pump system, Energ. Conver. Manage. 48 (11) (2007) 2853–2863.
[252] P. Farzanehkhameneh, M. Soltani, F.M. Kashkooli, M. Ziabasharhagh, Optimization and energy-economic assessment of a geothermal heat pump system, Renew. Sustain. Energy Rev. 133 (2020) 110282.
[253] M. Rivoire, A. Casasso, B. Piga, R. Sethi, Assessment of energetic, economic and environmental performance of ground-coupled heat pumps, Energies 11 (8) (2018) 1941.
[254] W. Lyu, X. Li, S. Yan, S. Jiang, Utilizing shallow geothermal energy to develop an energy efficient HVAC system, Renew. Energy 147 (2020) 672–682.
[255] R. Miao, X. Hu, Long-term monitoring and simulation of a vertical closed-loop ground source heat pump system used in the cold climate of the US, ASHRAE Trans. 125 (2019) 347–355.
[256] A. Cacabelos, P. Eguía, J.L. Míguez, E. Granada, M.E. Arce, Calibrated simulation of a public library HVAC system with a ground-source heat pump and a radiant floor using TRNSYS and GenOpt, Energ. Buildings 108 (2015) 114–126.
[257] S.M. Bina, H. Fujii, H. Kosukegawa, F. Inagaki, A predictive model of long-term performance assessment of Ground Source Heat Pump (GSHP) systems in Japanese regions, Geothermics 119 (2024) 102955.
[258] A. Cacabelos, P. Eguía, L. Febrero, E. Granada, Development of a new multi-stage building energy model calibration methodology and validation in a public library, Energ. Buildings 146 (2017) 182–199.
[259] X. Yuan, M. Zhu, Y. Liang, M. Shahrestani, R. Kosonen, Comparison of short and long-term energy performance and decarbonization potentials between cogeneration and GSHP systems under MARKAL scenarios, Sustainability 15 (2) (2023) 1604.
[260] A. Shah, M. Krarti, J. Huang, Energy performance evaluation of shallow ground source heat pumps for residential buildings, Energies 15 (3) (2022) 1025.
[261] J.I. Villarino, A. Villarino, F.Á. Fernández, Experimental and modelling analysis of an office building HVAC system based in a ground-coupled heat pump and radiant floor, Appl. Energy 190 (2017) 1020–1028.
[262] J. Xiong, C. Wang, S. Sun, C. Xu, Q. Mao, G. Li, Study of temperature sensors online fault-tolerant control for HVAC system using, EnergyPlus-Python co-simulation, 2023.

[263] K. Ahmed, J. Fadejev, J. Kurnitski, Modeling an alternate operational ground source heat pump for combined space heating and domestic hot water power sizing, Energies 12 (11) (2019) 2120.
[264] C. Piselli, J. Romanelli, M. Di Grazia, A. Gavagni, E. Moretti, A. Nicolini, F. Cotana, F. Strangis, H.J. Witte, A.L. Pisello, An integrated HBIM simulation approach for energy retrofit of historical buildings implemented in a case study of a medieval fortress in Italy, Energies 13 (10) (2020) 2601.
[265] D. Pahud, M. Belliardi, P. Caputo, Geocooling potential of borehole heat exchangers' systems applied to low energy office buildings, Renew. Energy 45 (2012) 197–204.
[266] F. Reda, A. Laitinen, Different strategies for long term performance of SAGSHP to match residential energy requirements in a cold climate, Energ. Buildings 86 (2015) 557–572.
[267] N. Vassileva, A. Georgiev, R. Popov, Simulation study of hybrid ground-source heat pump system with solar collectors, Bulg. Chem. Commun. 48 (2016) 71–76.
[268] S.K. Shah, L. Aye, B. Rismanchi, Multi-objective optimisation of a seasonal solar thermal energy storage system for space heating in cold climate, Appl. Energy 268 (2020) 115047.
[269] V. Ballerini, E. Rossi di Schio, P. Valdiserri, C. Naldi, M. Dongellini, A long-term dynamic analysis of heat pumps coupled to ground heated by solar collectors, Appl. Sci. 13 (13) (2023) 7651.
[270] S.O.D. Niaki, M. Pourfallah, A.Z. Ghadi, Feasibility and investigation of residential HVAC system with combined ground source heat pump and solar thermal collectors in different climates of Iran, International Journal of Thermofluids 20 (2023) 100427.
[271] F. Calise, F.L. Cappiello, M.D. d'Accadia, F. Petrakopoulou, M. Vicidomini, A solar-driven 5th generation district heating and cooling network with ground-source heat pumps: a thermo-economic analysis, Sustain. Cities Soc. 76 (2022) 103438.
[272] J.T. Good, V. Ismet Ugursal, A.S. Fung, Modeling and technical feasibility analysis of a low-emission residential energy system, Int. J. Green Energy 4 (1) (2007) 27–43.
[273] Y.-D. Jeong, M.G. Yu, Y. Nam, Feasibility study of a heating, cooling and domestic hot water system combining a photovoltaic-thermal system and a ground source heat pump, Energies 10 (8) (2017) 1243.
[274] Z. Wang, D. Huang, P. Wang, Q. Shen, Q. Zhang, Y. Sun, An analysis of solar heating system assisted by ground-source heat pumps in office building, Procedia Eng. 121 (2015) 1406–1412.
[275] S.M. Bina, H. Fujii, S. Tsuya, H. Kosukegawa, Comparative study of hybrid ground source heat pump in cooling and heating dominant climates, Energ. Conver. Manage. 252 (2022) 115122.
[276] G. Emmi, S. Bordignon, A. Zarrella, M. De Carli, A dynamic analysis of a SAGSHP system coupled to solar thermal collectors and photovoltaic-thermal panels under different climate conditions, Energ. Conver. Manage. 213 (2020) 112851.
[277] S.H. Razavi, R. Ahmadi, A. Zahedi, Modeling, simulation and dynamic control of solar assisted ground source heat pump to provide heating load and DHW, Appl. Therm. Eng. 129 (2018) 127–144.
[278] Y. Wen, S.-K. Lau, J. Leng, K. Liu, Sustainable underground environment integrating hybrid ventilation, photovoltaic thermal and ground source heat pump, Sustain. Cities Soc. 90 (2023) 104383.
[279] P. McKenna, W.J. Turner, D. Finn, Thermal energy storage using phase change material: Analysis of partial tank charging and discharging on system performance in a building cooling application, Appl. Therm. Eng. 198 (2021) 117437.
[280] C. Carmo, O. Dumont, M.P. Nielsen, B. Elmegaard, Energy Performance and Economic Evaluation of Heat Pump/Organic Rankine Cycle System with Sensible Thermal Storage, in: 29th International Conference on Efficiency, Cost, Optimization, Simulation and Environmental Impact of Energy Systems, 2016.
[281] Y. Wu, L. Hou, T. Su, Y. Ma, Simulation study on performance of solar-powered desiccant wheel and ground source heat pump air conditioning in Qingdao, Sustainability 16 (8) (2024) 3105.
[282] K. Fong, C. Lee, Investigation on hybrid system design of renewable cooling for office building in hot and humid climate, Energ. Buildings 75 (2014) 1–9.
[283] F. Busato, R. Lazzarin, M. Noro, The control of renewable energies to improve the performance of multisource heat pump systems: a two-case study, Appl. Sci. 11 (14) (2021) 6653.
[284] K. Fong, C. Lee, T. Zhao, Effective design and operation strategy of renewable cooling and heating system for building application in hot-humid climate, Sol. Energy 143 (2017) 1–9.
[285] A. Rosato, A. Ciervo, G. Ciampi, M. Scorpio, S. Sibilio, Impact of seasonal thermal energy storage design on the dynamic performance of a solar heating system serving a small-scale Italian district composed of residential and school buildings, J. Storage Mater. 25 (2019) 100889.
[286] E. Marrasso, C. Roselli, F. Tariello, Comparison of two solar PV-driven air conditioning systems with different tracking modes, Energies 13 (14) (2020) 3585.
[287] A. Dama, A. Angelotti, D. Penso, Integrated design and dynamic simulation for a new zero energy building, Proceedings-Building Simulation Applications BSA 2015 (2015) 223–230.
[288] A. Rosato, A. Ciervo, G. Ciampi, M. Scorpio, S. Sibilio, Integration of micro-cogeneration units and electric storages into a micro-scale residential solar district heating system operating with a seasonal thermal storage, Energies 13 (20) (2020) 5456.
[289] N. Ziozas, A. Kitsopoulou, E. Bellos, P. Iliadis, D. Gonidaki, K. Angelakoglou, N. Nikolopoulos, S. Ricciuti, D. Viesi, Energy performance analysis of the renovation process in an italian cultural heritage building, Sustainability 16 (7) (2024) 2784.
[290] A. Rosato, A. Ciervo, G. Ciampi, M. Scorpio, F. Guarino, S. Sibilio, Energy, environmental and economic dynamic assessment of a solar hybrid heating network operating with a seasonal thermal energy storage serving an Italian small-scale residential district: influence of solar and back-up technologies, Therm. Sci. Eng. Prog. 19 (2020) 100591.
[291] G. Stamatellos, O. Zogou, A. Stamatelos, Energy analysis of a NZEB office building with rooftop pv installation: Exploitation of the employees' electric vehicles battery storage, Energies 15 (17) (2022) 6206.
[292] M. Azaza, D. Eriksson, F. Wallin, A study on the viability of an on-site combined heat-and power supply system with and without electricity storage for office building, Energ. Conver. Manage. 213 (2020) 112807.
[293] A. Rosato, A. Ciervo, F. Guarino, G. Ciampi, M. Scorpio, S. Sibilio, Dynamic simulation of a solar heating and cooling system including a seasonal storage serving a small Italian residential district, Thermal Science, 24 (6 Part A) (2020) 3555-3568.
[294] C. Roselli, M. Sasso, F. Tariello, A wind electric-driven combined heating, cooling, and electricity system for an office building in two Italian cities, Energies 13 (4) (2020) 895.
[295] N. Ashrafi, R. Ahmadi, A. Zahedi, Technical, economical, and environmental scenario based modeling of the building equipped with ground source heat pump (GSHP) and solar system, Energ. Buildings 289 (2023) 113048.
[296] S. Bae, Y. Nam, I. da Cunha, Economic solution of the tri-generation system using photovoltaic-thermal and ground source heat pump for zero energy building (ZEB) realization, Energies 12 (17) (2019) 3304.
[297] N. Sommerfeldt, H. Madani, In-depth techno-economic analysis of PV/Thermal plus ground source heat pump systems for multi-family houses in a heating dominated climate, Sol. Energy 190 (2019) 44–62.
[298] Y. Ruoping, Y. Xiangru, Y. Xiaohui, B. Yunpeng, W. Huajun, Performance study of split type ground source heat pump systems combining with solar photovoltaic-thermal modules for rural households in North China, Energ. Buildings 249 (2021) 111190.
[299] A.A. Safa, A.S. Fung, R. Kumar, Comparative thermal performances of a ground source heat pump and a variable capacity air source heat pump systems for sustainable houses, Appl. Therm. Eng. 81 (2015) 279–287.
[300] S. Chang, G. Feng, L. Zhang, K. Huang, A. Li, Multi-objective optimization of a photovoltaic thermal curtain wall assisted dual-source heat pump system, Appl. Therm. Eng. 222 (2023) 119845.
[301] J. Zhu, Y. Tao, Comparative study among hybrid ground source heat pump system, complete ground source heat pump and conventional HVAC System, ASME International Mechanical Engineering Congress and Exposition (2011) 693–699.